AD-A054 093 NORTH CAROLINA STATE UNIV RALEIGH DEPT OF MECHANICAL--ETC F/G 20/4
INVESTIGATION OF A WING-ROTOR INTERACTION SYSTEM FOR HELICOPTER--ETC(U)
MAR 78 F R DEJARNETTE, N T FRINK, M A TAKALLU DAHC04-74-G-0007
ARO-11945.2-E NL

UNCLASSIFIED

| OF |
AD
A054093

END
DATE
FILMED
6-78
DDC

ARO 11945.2-E and 13573.2-E

INVESTIGATION OF A WING-ROTOR INTERACTION SYSTEM FOR HELICOPTERS.

FINAL REPORT.
1 Sep 73 - 31 Dec 77

by

Fred R. DeJarnette
Neal T. Frink
Mohammad A. Takallu
Steven L. Griffith
James J. Murray

6 March 1978

67p.

for

U. S. ARMY RESEARCH OFFICE
Research Triangle Park, N. C. 27709

GRANT NUMBERS
DAHC04-74-G-0007
DAHC04-75-G-0023
DAAG29-76-G-0045
DAAG29-76-G-0318

ARO, ARO
11945.2-E,
13573.2-E

Mechanical and Aerospace Engineering Department
NORTH CAROLINA STATE UNIVERSITY
RALEIGH, N. C. 27650

APPROVED FOR PUBLIC RELEASE;
DISTRIBUTION UNLIMITED

1473

400 714

LB

ROUTING AND TRANSMITTAL SLIP		ACTION
1 TO DDC	INITIALS	CIRCULATE
	DATE	COORDINATION
2	INITIALS	FILE
	DATE	INFORMATION
3	INITIALS	NOTE AND RETURN
	DATE	PER CONVERSATION
4	INITIALS	SEE ME
	DATE	SIGNATURE

REMARKS

This report is the final report for two projects sponsored by the Army Research Office. It, therefore, carries two monitor report numbers:

11945.2-E

and

13573.2-E

Do NOT use this form as a RECORD of approvals, concurrences, disapprovals, clearances, and similar actions

FROM	DATE
U. S. Army Research Office Post Office Box 12211 Research Triangle Park, NC 27709	9 May 78
	PHONE 935-3331 - AUTOVON

OPTIONAL FORM 41
AUGUST 1967
GSA FPMR (41CFR) 100-11.206

5041-101-01

* GPO : 1975-585-506

SECURITY CLASSIFICATION OF THIS PAGE (When Data Entered)

REPORT DOCUMENTATION PAGE		READ INSTRUCTIONS BEFORE COMPLETING FORM
1. REPORT NUMBER	2. GOVT ACCESSION NO.	3. RECIPIENT'S CATALOG NUMBER
4. TITLE (and Subtitle) INVESTIGATION OF A WING-ROTOR INTERACTION SYSTEM FOR HELICOPTERS		5. TYPE OF REPORT & PERIOD COVERED Final, 1 Sept. 1973 to 31 Dec. 1977 6. PERFORMING ORG. REPORT NUMBER
7. AUTHOR(s) Fred R. DeJarnette, Neal T. Frink, Mohammad A. Takallu, Steven L. Griffith, and James J. Murray		8. CONTRACT OR GRANT NUMBER(s) DAHC04-74-G-0007 DAHC04-75-G-0023 DAAG29-76-G-0045 DAAG29-76-G-0318
9. PERFORMING ORGANIZATION NAME AND ADDRESS Mechanical and Aerospace Engineering Department North Carolina State University Raleigh, North Carolina 27650		10. PROGRAM ELEMENT, PROJECT, TASK AREA & WORK UNIT NUMBERS
11. CONTROLLING OFFICE NAME AND ADDRESS U. S. Army Research Office Post Office Box 12211 Research Triangle Park, N. C. 27709		12. REPORT DATE March 6, 1978 13. NUMBER OF PAGES 63
14. MONITORING AGENCY NAME & ADDRESS(if different from Controlling Office)		15. SECURITY CLASS. (of this report) Unclassified 15a. DECLASSIFICATION/DOWNGRADING SCHEDULE

16. DISTRIBUTION STATEMENT (of this Report)

Approved for public release; distribution unlimited

17. DISTRIBUTION STATEMENT (of the abstract entered in Block 20, if different from Report)

NA

18. SUPPLEMENTARY NOTES

The findings in this report are not to be construed as an official Department of the Army position, unless so designated by other authorized documents.

19. KEY WORDS (Continue on reverse side if necessary and identify by block number)

20. ABSTRACT (Continue on reverse side if necessary and identify by block number)

This research includes experimental and analytical investigations to determine if favorable interference effects could be obtained from a wing-rotor interaction system. The experimental investigation was conducted in the North Carolina State University subsonic wind tunnel. Lift and drag forces were measured on a wing, mounted in a cantilevel fashion from the wall, and on a proprotor positioned above the wing on a shaft which ran through the ceiling of the test section. Test results showed significant increases in lift and →

next Page

DD FORM 1 JAN 73 1473 EDITION OF 1 NOV 65 IS OBSOLETE

SECURITY CLASSIFICATION OF THIS PAGE (When Data Entered)

20. ABSTRACT (continued)

decreases in drag for both the wing and the proprotor due to favorable interference effects.

The analytical investigation developed a new lifting surface theory for subsonic wings which can also be interpreted as a vortex lattice method. Results were found to be more accurate and converge faster than conventional vortex lattice methods. The accuracy compared well with other lifting surface theories, but with much smaller computational times.

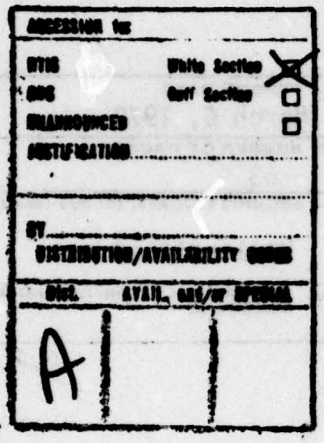

SUMMARY OF RESEARCH PERFORMED

The purpose of this research was to determine if favorable interference effects could be obtained from a wing-rotor interaction system. It was theorized by the fifth author, J. J. Murray, that when this system is in forward flight the oncoming stream would sweep the wake from the rotor over the top of the wing which would increase the velocity on the wing. The additional velocity passing over the top of the wing would decrease the pressure and increase the lift. This additional velocity would also delay boundary layer separation, increase the stall angle of attack, and decrease the drag.

This final report covers the research performed from September 1, 1973 to December 31, 1977. The first two years was devoted to an experimental investigation in the North Carolina State University Subsonic Wind Tunnel. A wing which spanned half of the test-section width was mounted in a cantilever fashion from a side wall, and the proprotor was positioned above the wing tip on a shaft which ran through the ceiling. The wing and proprotor were instrumented separately to measure their lift and drag, and one wing model was constructed to measure the pressure distribution. The test results showed significant increases in lift and decrease in drag for both the wing and the proprotor due to favorable interference effects. Measured pressure distributions on the wing revealed that the inpingement of the proprotor's wake delayed separation and thus increased the stall angle of the wing. A complete description of this investigation is given in the Master's thesis (ref. 1) of S. L. Griffith, fourth author. A condensed version was presented at the AIAA 3rd Atmospheric Flight Mechanics Conference held in Arlington, Texas, June 7-9, 1976 and appears in the proceedings of that conference (ref. 2).

The experimental investigations showed that the concept of favorable interference with the wing-rotor system was feasible and prompted an analytical investigation. In order to calculate the combined flow field of the rotor and the wing, it is necessary to have a method which will calculate subsonic wing properties accurately and expediously. The last two years of this research was devoted to this task.

The first author (ref. 3) developed a new lifting surface theory for rectangular wings. The solution can also be interpreted as a vortex lattice method; however, the optimum locations of horseshoe vortices and control points are determined in the solution. It properly locates the tip vortices to be inset from the wing tips which other investigators found empirically. The method of solution properly accounts for the leading-edge singularity, Cauchy singularity, and Kutta condition. Results were found to be more accurate and converge faster than conventional vortex lattice methods. In addition, the accuracy was found to be comparable to other lifting surface theories, but with much smaller computational times. This method was presented at the Vortex Lattice Utilization Workshop held at NASA Langley Research Center, May 17-18, 1976. A description of the technique used to extract the leading-edge suction parameter from the solution is given in reference 4, and it was also presented at 13th Annual Meeting of the Society of Engineering Science, Hampton, Virginia, November 1-3, 1976.

The first three authors extended the lifting surface theory to skewed and swept wings (ref. 5 attached to this report). The extension to skewed wings was straightforward; however, the midspan point of swept wings presented a problem. A "kink" in the spanwise vortex occurs there, and the theory must be modified in a fashion similar to that used by Multhopp in order to get a good solution. The spanwise variation of vorticity was calculated by two

methods, a Fourier sine series and a direct solution for the vorticity at specific spanwise locations. Both methods yielded essentially the same results for rectangular wings, but the Fourier sine series gave oscillatory results for the swept wing. In general, the direct method gave satisfactory results which compared well with other methods. A condensed version of reference 5 will be submitted to the Journal of Aircraft.

RECOMMENDATIONS

It is recommended that the analytical investigation be extended to include a rotor passing over the wing. A more accurate mathematical model of the wake should also be included.

REFERENCES

1. Griffith, S. L., "An Experimental Investigation of Favorable Interference Effects from a Wing and Proprotor," M. S. Thesis, N. C. State University, Raleigh, N. C. (April, 1976).

2. Griffith, S. L., DeJarnette, F. R. and Murray, J. J., "An Experimental Investigation of Favorable Interference Effects from a Wing and Proprotor," (Proceedings of AIAA 3rd Atmospheric Flight Mechanics Conference, Arlington, Texas, June 7-9, 1976), pp. 92-100.

3. DeJarnette, F. R., "Arrangement of Vortex Lattices on Subsonic Wings," NASA SP-405, pp. 301-324, (1976).

4. DeJarnette, F. R., "Lifting Surface Theory for Rectangular Wings," NASA CP-2001, Vol. 4, pp. 1301-1310 (1976).

5. Frink, N. T., Takallu, M. A. and DeJarnette, F. R., "Lifting Surface Theory for Skewed and Swept Subsonic Wings," North Carolina State University Report, March, 1978.

LIFTING SURFACE THEORY FOR SKEWED AND SWEPT SUBSONIC WINGS

by

Neal T. Frink
Mohammed A. Takallu
Fred R. DeJarnette

Mechanical and Aerospace Engineering Department
North Carolina State University
Raleigh, North Carolina 27650

Grant Number DAAG 29-76-G-0318

for

U. S. Army Research Office
Research Triangle Park, N. C. 27709

March, 1978

ACKNOWLEDGMENTS

The authors wish to thank the U. S. Army Research Office, Research Triangle Park, North Carolina for supporting this research under Grant Number DAAG 29-76-G-0318. The Grant Monitor was Mr. J. J. Murray, Director of the Engineering Sciences Division at the Army Research Office, and the Project Director was Dr. F. R. DeJarnette at North Carolina State University. The authors would also like to thank Ms. Deborah S. Clapp for typing the manuscript and assisting with the reproduction.

CONTENTS

1. SUMMARY

A new method is developed for solving the lifting surface equation for thin wings. The downwash equation is transformed into double integrals involving Cauchy-type singularities in the chordwise and spanwise directions. A technique developed by Lan for airfoil theory is used to reduce both integrals to a double summation. This method properly accounts for the leading-edge singularity, Cauchy singularity, and Kutta condition. The circulation is determined by solving the matrix equation formed by requiring the downwash equation to satisfy the tangent-flow boundary condition at specific control points on the wing. Two methods were used for the spanwise variation of the circulation: a Fourier-sine series and a direct matrix solution which determines the circulation at specific spanwise locations. These two methods were found to yield essentially the same results for rectangular and skewed wings. However, the direct matrix method gave more satisfactory results for swept wings. The differences are attributed to the infinite downwash caused by the "kink" in the spanwise vortices at the midspan of swept wings. The solutions generally compared well with other lifting-surface theories, but with much smaller computational times, and the method was found to be more accurate and converge faster than conventional vortex lattice methods.

2. INTRODUCTION

The motivation for the research described in this report stemmed from an experimental investigation of a wing-rotor interaction system for helicopters. A complete description of this investigation is given in reference 1, and a condensed version appears in reference 2. Subsonic wind tunnel tests were performed to determine the interference effects of a wing and proprotor on their lift and drag characteristics. A wing which spanned half of the test-section width was mounted in a cantilever fashion from a side wall, and the proprotor was positioned above the wing tip on a shaft which ran through the ceiling. The wing and proprotor were instrumented separately to measure their lift and drag, and one wing model was constructed to measure the pressure distribution. The test results showed significant increases in lift and decrease in drag for both the wing and the proprotor due to favorable interference effects. Measured pressure distributions on the wing revealed that the impingement of the proprotor's wake delayed separation and thus increased the stall angle of the wing. These features made the concept attractive for future design considerations and prompted the present analytical investigation of subsonic wings.

An analytical investigation of a complete wing rotor flow field requires computational methods for both the wing and the rotor. In order to calculate the combined flow field efficiently, it is necessary to have a method which will calculate subsonic wing properties accurately and expediously. It is the purpose of this report to develop such a method.

Aerodynamic characteristics of wings at subsonic speeds are generally calculated by vortex lattice or lifting surface methods. In the conventional vortex lattice method (VLM) the planform of the wing is divided into a number of elemental panels, and a horseshoe vortex is placed at the local quarter-

chord of each panel. The boundary condition is satisfied at the local three-quarter chord of each panel by requiring the flow to be tangent to the surface there. The strengths of the horseshoe vortices are determined by solving the matrix equation formed from the boundary-condition equations. Then the aerodynamic characteristics, such as lift, induced drag, pitching moment, and rolling moment are calculated by summing the results from each panel. A complete description of the vortex lattice method is given in reference 3. Vortex-lattice methods are simplier and easier to apply to complex configurations than lifting surface methods, but they are generally less accurate (ref. 4).

In lifting surface theories, a continuous loading or circulation in both the spanwise and chordwise directions is used to determine the aerodynamic characteristics of the wing. Here, singular integral equations must be solved which cause numerical difficulties. The load distribution is generally represented by a double series and the coefficients of these series are determined by solving the matrix equation which results from applying the tangent-flow boundary condition at specific points, called control points. Lifting-surface theories are discussed in reference 5.

Lan (ref. 4) developed an ingenious method for thin, two-dimensional airfoils by using the midpoint trapezoidal rule and the theory of Chebychev polynomials to reduce the downwash integral to a finite sum. This method is simple to apply and gives an accurate solution to the airfoil downwash equation. A more detailed description is given below. Lan also developed a quasi-vortex lattice method for finite wings by using his airfoil method for a continuous chordwise vortex distribution in the spanwise direction. The results showed an improvement over the conventional vortex lattice method. An additional improvement was found empirically by Hough (ref. 6) when the lattice was inset 1/4 of a lattice width at the wing tips.

DeJarnette (ref. 7) developed a new lifting surface theory for rectangular wings which uses Lan's continuous chordwise vortex distribution but, unlike Lan, a continuous spanwise vortex distribution also. Although the vortex distributions are continuous, the method is easily interpreted as a vortex lattice method in which the arrangement of horseshoe vortices and control points are determined from the solution rather than chosen like the conventional vortex lattice method. It properly locates the tip vortices to be inset from the wing tips like Hough (ref. 6) found empirically. The results were found to compare very closely with other lifting surface theories, but the computational time was only about 1/10 of the other methods. The results were more accurate and converged much more rapidly than the vortex lattice method of reference 3. A description of the method used for extracting the leading-edge suction parameter from the solution is given in reference 8.

The lifting surface theory given in references 7 and 8 apply the downwash integral in the form involving Cauchy singularities rather than the Mangler singularity form which is usually used in lifting surface theories. Consequently, difficulties are encountered when the same method is applied to non-rectangular planforms. This report develops a generalized lifting surface theory which can be applied to wings which are skewed, swept, or tapered, yet it retains the same accuracy and simplicity as the method given in references 7 and 8.

3. SYMBOLS

A	parameter defined by eq. (7.13)
A'	parameter defined by eq. (7.26)
A_{kn}	unknowns in the downwash matrix
A_s	parameter defined by eq. (6.10)
A_{sk}	parameter defined by eq. (6.14)
A_1	parameter defined by eq. (8.12)
$\overline{A}_1$	parameter defined by eq. (B-3)
A_2	parameter defined by eq. (8.19)
AR	aspect ratio
b	wing span
B	parameter defined by eq. (7.14)
B'	parameter defined by eq. (7.27)
B_s	parameter defined by eq. (6.11)
B_{sk}	parameter defined by eq. (6.15)
B_1	parameter defined by eq. (8.13)
$\overline{B}_1$	parameter defined by eq. (B-4)
B_2	parameter defined by eq. (8.20)
c	wing chord
$\overline{c}$	mean chord of wing
c_R	wing root chord
c_T	wing tip chord
c_{TL}	left wing tip chord
c_{TR}	right wing tip chord
C_ℓ	sectional lift coefficient
C_L	wing lift coefficient

C_{L_α}	lift curve slope, per radian
C_m	sectional moment coefficient
C_M	wing pitching moment coefficient, about leading edge at midspan
C_s	leading edge suction parameter
d	parameter defined by eq. (7.10)
d'	parameter defined by eq. (7.23)
e	parameter defined by eq. (7.11)
e'	parameter defined by eq. (7.24)
f	parameter defined by ew. (7.12)
f'	parameter defined by eq. (7.25)
G	parameter defined by eq. (5.8)
$K_{ijk\ell}$	parameter defined by eq. (6.13)
$K_{L_{ijk\ell}}$	parameter defined by eq. (8.18)
$K_{LC_{ijk\ell}}$	parameter defined by eq. (8.16)
$K_{R_{ijk\ell}}$	parameter defined by eq. (8.11)
$\bar{K}_R$	parameter defined by eq. (B-2)
$K_{RC_{ijk\ell}}$	parameter defined by eq. (8.9)
m_{LE}	$\tan \Lambda_{LE}$
m_{TE}	$\tan \Lambda_{TE}$
Δm	$\tan \Lambda_{TE} - \tan \Lambda_{LE}$
M	number of spanwise vortices
n	summational integer
N	number of chordwise vortices and control points
S	wing planform area
u,v	parameters for integration by parts, see eq. (7.4)
VLM	vortex lattice method

V_∞	freestream velocity
w	downwash velocity, positive upward
w_L	downwash velocity induced by the vortices on left wing panel
w_{LC}	downwash velocity induced by the left vortex filament at the wing midspan
w_R	downwash velocity induced by the vortices on right wing panel
w_{RC}	downwash velocity induced by the right vortex filament at the wing midspan
x	chordwise coordinate measured from leading edge in direction of V_∞
X	parameter defined by eq. (6.9)
X_{ac}	wing aerodynamic center location
y	spanwise coordinate on right wing panel, positive to the right
$\bar{y}$	spanwise coordinate on left wing panel
Y	parameter defined by eq. (7.8)
Y'	parameter defined by eq. (7.21)
Y_0	parameter defined by eq. (7.9)
Y_0'	parameter defined by eq. (7.22)
z_c	vertical coordinate of mean camber line
α	angle of attack
γ	non-dimensional circulation per unit chord
Γ	circulation
δ_i^k	parameter defined by eq. (9.18)
η	non-dimensional chordwise coordinate, see eq. (6.2)
θ	transformed chordwise coordinate
λ	wing taper ratio
Λ_{LE}	leading edge sweep
Λ_{TE}	trailing edge sweep
ϕ	transformed spanwise coordinate on right wing panel

$\overline{\phi}$	transformed spanwise coordinate on left wing panel
ϕ^*	transformed spanwise coordinate for entire span, see eqs. (8.2) and (8.3)

Subscripts

i	chordwise control point, see eq. (4.7)
j	spanwise control point, see eq. (5.14)
k	chordwise vortex point, see eq. (4.6)
ℓ	spanwise vortex point, see eq. (5.13)
LE	leading edge of wing
TE	trailing edge of wing

4. LAN'S TWO-DIMENSIONAL THEORY

For thin airfoils, the downwash equation is

$$w_i = -\frac{1}{2\pi}\int_0^c \frac{\gamma(x_1)\,dx_1}{x_i - x_1} . \tag{4.1}$$

The integral on the right side is of the Cauchy type, and the integrand has a singularity at $x_1 = x_i$. Transform the x coordinate by

$$x/c = (1 - \cos\theta)/2 \tag{4.2}$$

and use the following result from airfoil theory (ref. 9)

$$\int_0^\pi \frac{d\theta_1}{\cos\theta_1 - \cos\theta} = 0 \tag{4.3}$$

to write eq. (4.1) as

$$w_i = -\frac{1}{2\pi}\int_0^\pi \frac{\gamma(\theta_1)\sin\theta_1\,d\theta_1}{\cos\theta_1 - \cos\theta} = -\frac{1}{2\pi}\int_0^\pi \frac{[\gamma(\theta_1)\sin\theta_1 - \gamma(\theta)\sin\theta]\,d\theta_1}{\cos\theta_1 - \cos\theta} \tag{4.4}$$

Now the singularity in the integrand has been removed because the numerator approaches zero at the same position ($\theta_1 = \theta$) that the denominator approaches zero.

Lan (ref. 4) used the theory of Chebychev polynomials to show that

$$\sum_{k=1}^{N} \frac{1}{\cos\theta_k - \cos\theta_i} = \begin{cases} -N^2 & \text{for } i = 0 \\ 0 & \text{for } i \neq 0, N \\ N^2 & \text{for } i = N \end{cases} \tag{4.5}$$

when the vortex positions are

$$\theta_k = \frac{(2k - 1)\pi}{2N} , \quad k = 1, \ldots, N \tag{4.6}$$

and the control points are located at

$$\theta_i = \frac{i\pi}{N} , \quad i = 0, 1, \ldots, N . \tag{4.7}$$

Then the integral in eq. (4.4) can be reduced to a finite sum by using the midpoint trapezoidal rule (ref. 4) and eq. (4.5) to obtain

$$w_i = -\frac{1}{2\pi}\frac{\pi}{N}\sum_{k=1}^{N}\frac{\gamma_k \sin\theta_k - \gamma_i \sin\theta_i}{\cos\theta_k - \cos\theta_i}$$

$$= -\frac{1}{2N}\sum_{k=1}^{N}\frac{\gamma_k \sin\theta_k}{\cos\theta_k - \cos\theta_i} + \begin{cases} -\frac{N}{2}\lim\limits_{\theta\to 0}\gamma(\theta)\sin\theta , & i = 0 \\ 0 , & i \neq 0, N \\ \frac{N}{2}\lim\limits_{\theta\to\pi}\gamma(\theta)\sin\theta , & i = N \end{cases} \tag{4.8}$$

However,

$$\lim_{\theta\to 0}\gamma(\theta)\sin\theta = 4\,C_S \tag{4.9}$$

where C_S is the leading-edge suction parameter and since the Kutta condition requires that $\gamma(\pi) = 0$,

$$\lim_{\theta\to\pi}\gamma(\theta)\sin\theta = 0. \tag{4.10}$$

Unlike the conventional vortex lattice method, the Cauchy singularity, leading-edge square-root singularity and the Kutta condition are properly accounted for in this method. Equation (4.8) can be solved with $i \neq 0$ to obtain the N values of γ_k, and then the leading-edge suction parameter can be computed by using eq. (4.8) with $i = 0$ (control point at the leading edge). Figure 1 illustrates the positions of the vortices and control points by the "semi-circle method" for $N = 2$. With only one vortex ($N = 1$) on a flat plate, the exact lift and leading-edge suction are obtained, and the Kutta condition is satisfied. With two or more vortices

the exact pitching moment is obtained in addition to the above properties and the calculated γ_k are exact. It can be shown that the remarkable accuracy of this method is due to eq. (4.5), which is similar to the integral result given by eq. (4.3) and used in exact thin airfoil theory.

5. PRANDTL'S LIFTING-LINE THEORY

Before developing the lifting surface equations for skewed and swept wings, the technique for performing the spanwise integration will be tested with Prandtl's lifting-line equation. The lifting-line equation is given by ref. 9 as

$$\Gamma = \pi V_\infty c \left[\alpha - \frac{1}{4\pi V_\infty} \int_{-b/2}^{b/2} \frac{d\Gamma}{dy_1} \frac{dy_1}{(y-y_1)} \right] \tag{5.1}$$

This equation has a Cauchy type integral on the right side, and therefore the method used by Lan for the airfoil is applicable. In reference 7 the spanwise coordinate was transformed by the "semi-circle" method

$$y = -\frac{b}{2} \cos \phi \tag{5.2}$$

and the circulation $\Gamma(\phi)$ was represented by Multhopp's interpolation formula which is a Fourier sine series. Then Lan's airfoil technique was used to solve equation (5.1). The results were found to be identical to the classical solution of Prandtl's lifting-line equation (ref. 9).

When using the Fourier sine series for Γ in eq. (5.1), the series must be differentiated and the accuracy of the resulting series is questionable. Instead of using a series for Γ, values of the derivative of Γ at discrete spanwise locations will be calculated here. When treating swept wings in Chapter 7, it will be necessary to divide the spanwise

integration range into a left-wing panel and a right-wing panel. Therefore, for the analysis here the spanwise coordinate will be transformed by applying the "semi-circle" method to each wing panel separately. As shown in Appendix A, the transformation given by eq. (5.2) is replaced by the following:

$$y = \frac{b}{4}(1 - \cos\phi) \text{ for } y > 0 \quad \text{(right-wing panel)} \tag{5.3}$$

and

$$\bar{y} = -\frac{b}{4}(1 - \cos\bar{\phi}) \text{ for } y < 0 \text{ (left-wing panel)} \tag{5.4}$$

The downwash integral in eq. (5.1) can be divided into a contribution from the left-wing panel and right-wing panel.

$$w_j = w_{R_j} + w_{L_j}$$

and for $y_j > 0$,

$$w_{R_j} = -\frac{1}{4\pi V_\infty}\int_0^{b/2}\frac{d\Gamma}{dy_1}\frac{dy_1}{(y_j - y_1)} = -\frac{1}{4\pi V_\infty}\frac{4}{b}\int_0^{\pi}\frac{d\Gamma}{d\phi}\frac{d\phi_1}{(\cos\phi_1 - \cos\phi_j)} \tag{5.6}$$

and

$$w_{L_j} = -\frac{1}{4\pi V_\infty}\int_{-b/2}^{0}\frac{d\Gamma}{d\bar{y}_1}\frac{d\bar{y}_1}{(y_j - \bar{y}_1)} = -\frac{1}{4\pi V_\infty}\frac{4}{b}\int_{\pi}^{0}\frac{d\Gamma}{d\bar{\phi}_1}\frac{d\bar{\phi}_1}{(2 - \cos\phi_j - \cos\bar{\phi}_1)} \tag{5.7}$$

Note that eq. (5.6) has the Cauchy-type singularity but eq. (5.7) does not have a singularity in the integrand because $y_j > 0$ and the integral covers the left-wing panel where $\bar{y}_1 < 0$. With

$$G(\phi) = \frac{d\Gamma}{d\phi} \tag{5.8}$$

a wing symmetrically loaded about the midspan line ($y = 0$) will have

$$G(\bar{\phi}) = G(\phi) \tag{5.9}$$

and thus equation (5.7) can be written as

$$w_{L_j} = \frac{1}{\pi V_\infty b} \int_0^\pi \frac{G(\phi_1)\, d\phi_1}{(2 - \cos\phi_j - \cos\phi_1)} \tag{5.10}$$

Now replace eqs. (5.6) and (5.10) with the midpoint trapezoidal rule summation to get

$$w_{R_j} \simeq -\frac{1}{V_\infty b M} \sum_{\ell=1}^{M} \frac{G_\ell}{(\cos\phi_\ell - \cos\phi_j)} \tag{5.11}$$

and

$$w_{L_j} \simeq \frac{1}{V_\infty b M} \sum_{\ell=1}^{M} \frac{G_\ell}{(2 - \cos\phi_j - \cos\phi_\ell)} \tag{5.12}$$

These two equations represent the downwash due to trailing vortices located at

$$\bar{\phi}_\ell = \phi_\ell = \frac{(2\ell - 1)\pi}{2M}, \quad \ell = 1, \ldots, M \tag{5.13}$$

with control points located at

$$\phi_j = \frac{j\pi}{M}, \quad j = 0, 1, \ldots, M-1 \tag{5.14}$$

Since the downwash is expressed in terms of the unknown $G_\ell = (d\Gamma/d\phi)_\ell$, it is necessary to express Γ in terms of G before a solution to eq. (5.1) can be obtained. Noting that $\Gamma = 0$ at the wing tips, replace Γ by

$$\Gamma(\phi) = \int_\pi^\phi \frac{d\Gamma}{d\phi_1}\, d\phi_1 \tag{5.15}$$

and approximate the integral by the midpoint trapezoidal rule to get

$$\Gamma_j \simeq -\frac{\pi}{M} \sum_{\ell=j+1}^{M} G_\ell \tag{5.16}$$

Finally, substitute eqs. (5.11), (5.12), and (5.16) into (5.1) to obtain

$$\frac{b}{c_j} \sum_{\ell=j+1}^{M} G_\ell + \sum_{\ell=1}^{M} G_\ell \left[\frac{1}{2 - \cos\phi_\ell - \cos\phi_j} - \frac{1}{\cos\phi_\ell - \cos\phi_j} \right]$$

$$= -\alpha V_\infty M b \tag{5.17}$$

Apply eq. (5.17) at the spanwise locations $\phi_j (j = 0,1, \ldots, M-1)$ to obtain a matrix equation for the M values of $G_\ell (\ell = 1, \ldots, M)$. Then the aerodynamic coefficients can be calculated by reducing the spanwise integrals to a finite sum through the midpoint trapezoidal rule. For example, the lift coefficient is given by

$$C_L = \frac{2V_\infty}{S} \int_{-b/2}^{b/2} \Gamma \, dy_1 = \frac{V_\infty b}{S} \int_0^\pi \Gamma \sin\phi_1 \, d\phi_1 \tag{5.18}$$

Integrate the right side by parts to get

$$C_L = \frac{V_\infty b}{S} \left[\Gamma_{\phi=0} - \int_0^\pi \frac{d\Gamma}{d\phi_1} \cos\phi_1 \, d\phi_1 \right] \tag{5.19}$$

Replace the right side by the midpoint trapezoidal rule to get

$$C_L \simeq \frac{V_\infty b}{S} \left[-\frac{\pi}{M} \sum_{\ell=1}^{M} G_\ell - \frac{\pi}{M} \sum_{\ell=1}^{M} G_\ell \cos\phi_\ell \right] \tag{5.20}$$

Other aerodynamic coefficients can be calculated in a similar fashion.

6. LIFTING SURFACE THEORY FOR RECTANGULAR AND SKEWED WINGS

The downwash equation from lifting surface theory (ref. 10), in the Mangler integral form, is

$$w(x,y) = \frac{1}{4\pi} \iint_S \frac{\gamma(x_1,y_1)}{(y-y_1)^2} \left[1 + \frac{x-x_1}{\sqrt{(x-x_1)^2+(y-y_1)^2}} \right] dx_1 \, dy_1 \qquad (6.1)$$

Eq. (6.1) can be generalized to include skewed wings with taper by transforming the independent variables from x,y to η,y where

$$\eta(x,y) \equiv \frac{x-x_{LE}(y)}{c(y)} \qquad (6.2)$$

is the nondimensional chordwise variable ($0 \leq \eta \leq 1$). Thus,

$$x = x_{LE}(y) + \eta \, c(y) \qquad (6.3)$$

and eq. (6.1) becomes

$$w(\eta,y) = \frac{1}{4\pi} \iint \frac{\gamma(\eta_1,y_1)}{(y-y_1)^2} \, c(y_1) \left[1 + \frac{x-x_1}{\sqrt{(x-x_1)^2+(y-y_1)^2}} \right] d\eta_1 \, dy_1 \qquad (6.4)$$

where $x = x(\eta,y)$.

Equation (6.4) is not a Cauchy-type integral due to the term $(y-y_1)^2$ in the denominator. In order to apply Lan's two-dimensional method for the chordwise integration and the lifting-line method for the spanwise integration, eq. (6.4) must be transformed into a Cauchy-type integral form. To make this transformation, it is necessary to define the geometry and coordinate system of the skewed wing as shown in figure 2, and then integrate eq. (6.4) by parts in the spanwise direction.

Defining $m_{LE} \equiv \tan \Lambda_{LE}$, $m_{TE} \equiv \tan \Lambda_{TE}$, and $\Delta m \equiv m_{TE} - m_{LE}$, the geometry is described by

$$x_{LE} = y\, m_{LE}\,, \qquad x_{TE} = y\, m_{TE} + c_R \tag{6.5}$$

$$c(y) = x_{TE} - x_{LE}$$

$$= y\Delta m + c_R \tag{6.6}$$

where $c_R = \frac{b}{AR}$, $\Delta m = \frac{2(\lambda-1)}{AR(\lambda+1)}$, and $\lambda = \frac{c_{TR}}{c_{TL}}$.

Substitute eqs. (6.5) and (6.6) into eq. (6.3) to get

$$x = y\, m_{LE} + \eta[y\Delta m + c_R] \tag{6.7}$$

Substitute eq. (6.7) into eq. (6.4) and integrate by parts in the spanwise direction. *The downwash equation then becomes*

$$w(\eta,y) = -\frac{1}{4\pi} \int_0^1 \int_{-b/2}^{b/2} \left(\frac{\partial(\gamma c)}{\partial y_1}\right)_{\eta_1} \frac{1}{y-y_1} \left[1 + \frac{\sqrt{X}}{B_s}\right] dy_1\, d\eta_1 \tag{6.8}$$

where

$$X = (A_s^2 + 1)\,(y-y_1)^2 + 2A_s\, B_s\,(y-y_1) + B^2 \tag{6.9}$$

and

$$A_s = m_{LE} + \eta_1 \Delta m \tag{6.10}$$

$$B_s = (\eta-\eta_1)(c_R + y\Delta m) \tag{6.11}$$

Equation (6.8) contains Cauchy-type integrals, and it is therefore in the form to apply Lan's technique. With $y = -b/2 \cos \phi$ and $\eta = (1-\cos \theta)/2$, replace both integrals in eq. (6.8) with the midpoint trapezoidal-rule sum to get

$$w_{i,j} \simeq \frac{-1}{4\pi AR} \frac{\pi}{M} \frac{\pi}{N} \sum_{\ell=1}^{M} \sum_{k=1}^{N} \left[\frac{\partial \left(\frac{\gamma c}{c_R} \right)}{\partial \phi_1} \right]_{k,\ell} \frac{K_{ijk\ell} \cdot \sin \theta_k}{\cos \phi_\ell - \cos \phi_j} \tag{6.12}$$

where

$$K_{ijk\ell} \equiv 1 + \frac{\sqrt{(A_{sk}^2+1)(\cos \phi_\ell - \cos \phi_j)^2 + 2A_{sk} B_{sk} (\cos \phi_\ell - \cos \phi_j) + B_{sk}^2}}{B_{sk}} \tag{6.13}$$

and

$$A_{sk} = m_{LE} + \frac{\Delta m}{2} (1 - \cos \theta_k) \tag{6.14}$$

$$B_{sk} = (\cos \theta_k - \cos \theta_i)\left(\frac{1}{AR} - \frac{\Delta m}{2} \cos \phi_j\right) \tag{6.15}$$

The control points are located at

$$\theta_i = \frac{i\pi}{N}, \quad i = 1, \ldots, N \qquad \text{(chordwise)} \tag{6.16}$$

and

$$\phi_j = \frac{j\pi}{M}, \quad j = 1, \ldots, M-1 \qquad \text{(spanwise)} \tag{6.17}$$

and the integration or vortex points are located at

$$\theta_k = \frac{(2k-1)\pi}{2N}, \quad k = 1, \ldots, N \qquad \text{(chordwise)} \tag{6.18}$$

$$\phi_\ell = \frac{(2\ell-1)\pi}{2M}, \quad \ell = 1, \ldots, M \qquad \text{(spanwise)} \tag{6.19}$$

The spanwise variation of $\gamma_k(\phi)$ at the chordwise point θ_k is represented by a Fourier sine series

$$\frac{\gamma_k c}{c_R} = \sum_{n=1}^{M-1} A_{k,n} \sin n \phi \tag{6.20}$$

where $A_{k,n}$ are unknown parameters.

Substitute eq. (6.20) into eq. (6.8) to get the final form of the downwash as

$$w_{i,j} = \frac{-\pi}{4ARMN} \sum_{\ell=1}^{M} \sum_{k=1}^{N} \sum_{n=1}^{M-1} \frac{A_{kn} \cdot n \cdot \cos(n\phi_\ell) \cdot K_{ijk\ell} \sin \theta_k}{\cos \phi_\ell - \cos \phi_j} \tag{6.21}$$

The tangent flow boundary condition for thin wings requires that

$$w_{i,j} = \left(\frac{\partial z_c}{\partial x}\right)_{i,j} - \alpha \tag{6.22}$$

where $z_c(x,y)$ is the shape of the mean camber line. The N(M-1) values of $A_{k,n}$ are calculated by applying eq. (6.21) at the chordwise and spanwise control points given by eqs. (6.16) and (6.17) and solving the resulting matrix equation. For rectangular wings, only the odd values of n are needed because symmetry properties make the even coefficients zero. However, it is necessary to calculate the $A_{k,n}$ for both odd and even values of n for the skewed wing since the spanwise variation of circulation is not symmetric. After the $A_{k,n}$ are calculated, the circulation γ_k are determined by eq. (6.20). Regardless of the number (N) of chordwise vortices used, there is always a control point at the trailing edge which satisfies the Kutta condition.

The sectional and wing aerodynamic characteristics may now be calculated by using the midpoint trapezoidal rule to reduce the integrals to finite sums, as shown below.

$$(C_\ell)_j = \frac{2\Gamma_j}{cV_\infty} = \frac{2}{c} \int_0^c \gamma_j(x_1)\, dx_1 \simeq \frac{\pi}{N} \sum_{k=1}^{N} \gamma_{k,j} \sin \theta_k \tag{6.23}$$

$$C_L = \int_{-b/2}^{b/2} C_\ell \, c \, dy/S \simeq \frac{\pi}{2M} \sum_{j=1}^{M-1} (C_\ell)_j \left[1 - \frac{\Delta m AR}{2} \cos \phi_j\right] \sin \phi_j \qquad (6.24)$$

$$(C_m)_j = \frac{-2}{c^2} \int_0^c \gamma_j(x_1) \, x_1 \, dx_1 \simeq \frac{\pi}{2N} \sum_{k=1}^{N} \gamma_{k,j} \, (1 - \cos \theta_k) \sin \theta_k \qquad (6.25)$$

$$C_M = \int_{-b/2}^{b/2} C_m \, c^2 \, dy/S\bar{c} \simeq \frac{\pi}{2M} \sum_{j=1}^{M-1} (C_m)_j \, (1 - \cos \theta_k) \sin \theta_k \qquad (6.26)$$

$$(\bar{x}ac/c)_j = -(C_m/C_\ell)_j \qquad (6.27)$$

$$\bar{x}ac/\bar{c} = -C_M/C_L \qquad (6.28)$$

7. LIFTING SURFACE THEORY FOR SWEPT WINGS

The downwash equation for tapered wings, eq. (6.4), is

$$w(\eta,y) = \frac{1}{4\pi} \iint_S \frac{\gamma(\eta_1,y_1)}{(y-y_1)^2} \, c(y_1) \left[1 + \frac{x-x_1}{\sqrt{(x-x_1)^2+(y-y_1)^2}}\right] d\eta_1 \, dy_1 \qquad (7.1)$$

where $x = x_{LE}(y) + \eta c(y)$. (7.2)

It is important to note that eq. (7.1) is restricted to planforms with continuous vortex lines. The geometry of the swept wing does not allow continuous vortex lines in the spanwise direction because of a kink at the midspan, as shown in figure 3. Therefore, for the swept wing, eq. (7.1) is applied separately to the right wing panel and left wing panel.
Eq. (7.1) is of the Mangler integral form and must be integrated by parts to obtain the Cauchy-type integral forms which is necessary to apply Lan's

numerical method. The total downwash at (η,y) on the swept wing is, therefore, composed of the contribution from the left and right wing panels.

$$w(\eta,y) = \frac{1}{4\pi}\int_0^1\int_0^{b/2} \frac{\gamma(\eta_1,y_1)}{(y-y_1)^2}\, c(y_1) \left[1 + \frac{x-x_1}{\sqrt{(x-x_1)^2+(y-y_1)^2}}\right] dy_1\, d\eta_1$$

$$+ \frac{1}{4\pi}\int_0^1\int_{-b/2}^{0} \frac{\gamma(\eta_1,\bar{y}_1)}{(y-\bar{y}_1)^2}\, c(\bar{y}_1) \left[1 + \frac{x-x_1}{\sqrt{(x-x_1)^2+(y-\bar{y}_1)^2}}\right] d\bar{y}_1\, d\eta_1 \quad (7.3)$$

where $x = x(\eta,y)$ and $x_1 = x_1(\eta_1,y_1)$. Note that y_1 and $\bar{y}_1$ are the spanwise integration points for the right and left wing panels, respectively, and y is the spanwise position of a control point. Due to symmetry, control points are needed on one wing panel only, and the right wing panel is used here.

Considering the integrals in eq. (7.3) separately, the first integral is integrated by parts in the y_1-direction, holding η constant, with $y_1 > 0$ and $y > 0$, as follows:

$$\int_0^{b/2} udv = uv\Big|_0^{b/2} - \int_0^{b/2} vdu \quad (7.4)$$

where

$$u \equiv \gamma c \quad \text{and} \quad du = \left|\frac{\partial(\gamma c)}{\partial y_1}\right|_{\eta_1} dy_1 \quad (7.5)$$

$$dv \equiv \frac{1}{(y-y_1)^2}\left[1 + \frac{x-x_1}{\sqrt{(x-x_1)^2+(y-y_1)^2}}\right] dy_1 \quad (7.6)$$

$$v = \frac{1}{y-y_1} \left[1 + \frac{\sqrt{Y}}{B}\right] \tag{7.7}$$

The intermediate parameters are defined as

$$Y = d(y-y_1)^2 + e(y-y_1) + f \tag{7.8}$$

$$Y_0 = dy^2 + ey + f \tag{7.9}$$

$$d = A^2 + 1 \tag{7.10}$$

$$e = 2AB \tag{7.11}$$

$$f = B^2 \tag{7.12}$$

$$A = m_{LE} + \eta_1 \, \Delta m \tag{7.13}$$

$$B = (\eta-\eta_1)(c_R + y\Delta m)) \tag{7.14}$$

$$m_{LE} = \tan \Lambda_{LE} \tag{7.15}$$

$$\Delta m = \tan \Lambda_{TE} - \tan \Lambda_{LE} \tag{7.16}$$

Therefore, the spanwise part of the first integral is

$$\int_0^{b/2} udv = \frac{1}{4\pi} \frac{\gamma(\eta_1, y_1)\, c(y_1)}{y-y_1} \left[1 + \frac{\sqrt{Y}}{B}\right]_0^{b/2}$$

$$- \frac{1}{4\pi} \int_0^{b/2} \left[\frac{\partial(\gamma c)}{\partial y_1}\right]_{\eta_1} \frac{1}{y-y_1} \left[1 + \frac{\sqrt{Y}}{B}\right] dy_1 \tag{7.17}$$

The circulation γ at the wing tip, $y_1 = b/2$, is zero. Integrate eq. (7.17) in the chordwise direction to obtain

$$w_{RC}(\eta,y) + w_R(\eta,y) = -\frac{1}{4\pi}\int_0^1 \frac{\gamma(\eta_1,0)}{y} c_R \left[1 + \frac{\sqrt{Y_0}}{B}\right] d\eta_1$$

$$-\frac{1}{4\pi}\int_0^1\int_0^{b/2} \left[\frac{\partial(\gamma c)}{\partial y_1}\right] \frac{1}{y-y_1} \left[1 + \frac{\sqrt{Y}}{B}\right] dy_1\, d\eta_1 \qquad (7.18)$$

where w_{RC} and w_R are the downwash components for the right wing panel corresponding to the first and second integrals on the right side of eq. (7.18). The term w_R is the downwash from the vortices distributed over the right wing panel, while the term w_{RC} is the downwash from a vortex filament positioned at mid-span (y = 0).

Now, integrate the second integral term in eq. (7.3) by parts in the $\bar{y}_1$-direction, holding η constant, with $\bar{y}_1 < 0$ and $y > 0$, as follows

$$\int_{-b/2}^{0} u\,dv = uv\Big|_{-b/2}^{0} - \int_{-b/2}^{0} v\,du \qquad (7.19)$$

where $u \equiv \gamma c$ and $du = \left[\frac{\partial(\gamma c)}{\partial \bar{y}_1}\right]_{\eta_1} d\bar{y}_1$

$$dv \equiv \frac{1}{(y-\bar{y}_1)^2}\left[1 + \frac{x-x_1}{\sqrt{(x-x_1)^2+(y-\bar{y}_1)^2}}\right] d\bar{y}_1 \qquad (7.20)$$

$$v = \frac{1}{y-\bar{y}_1}\left[1 + \frac{\sqrt{Y'}}{B'}\right]$$

The intermediate parameters are defined as

$$Y' = d'(y-\bar{y}_1)^2 + e'(y-\bar{y}) + f' \qquad (7.21)$$

$$Y'_0 = d'y^2 + e'y + f' \qquad (7.22)$$

$$d' = (A')^2 + 1 \tag{7.23}$$

$$e' = 2A'B' \tag{7.24}$$

$$f' = (B')^2 \tag{7.25}$$

$$A' = -\Delta m \eta_1 - m_{LE} \tag{7.26}$$

$$B' = [2m_{LE} + \Delta m(\eta+\eta_1)]\, y + (\eta-\eta_1)\, c_R \tag{7.27}$$

Therefore, the spanwise part of the second integral term is

$$\int_{-b/2}^{0} udv = \frac{1}{4\pi} \frac{\gamma(\eta_1,\bar{y}_1)\, c(\bar{y}_1)}{y-\bar{y}_1} \left[1 + \frac{\sqrt{Y'}}{B'}\right]_{-b/2}^{0}$$

$$- \frac{1}{4\pi} \int_{-b/2}^{0} \left[\frac{\partial(\gamma c)}{\partial \bar{y}_1}\right]_{\eta_1} \frac{1}{y-\bar{y}_1} \left[1 + \frac{\sqrt{Y'}}{B'}\right] d\bar{y}_1 \tag{7.28}$$

Again, the circulation at the wing tip, $\bar{y}_1 = -b/2$, is $\gamma = 0$. Integrate eq. (7.28) in the chordwise direction to obtain

$$w_{LC}(\eta,y) + w_L(\eta,y) = + \frac{1}{4\pi} \int_0^1 \frac{\gamma(\eta_1,0)}{y} c_R \left[1 + \frac{\sqrt{Y'_0}}{B'}\right] d\eta_1$$

$$- \frac{1}{4\pi} \int_0^1 \int_{-b/2}^{0} \left[\frac{\partial(\gamma c)}{\partial \bar{y}_1}\right] \frac{1}{y-\bar{y}_1} \left[1 + \frac{\sqrt{Y'}}{B'}\right] d\bar{y}_1\, d\eta_1 \tag{7.29}$$

where w_{LC} and w_L are the downwash components for the left wing panel corresponding to the first and second integrals on the right side of eq. (7.29). The term w_L is the downwash from the vortices distributed over the left wing panel, while the term w_{LC} is the downwash from a vortex filament positioned at mid span.

The total downwash at (n,y) for the swept wing is now determined by substituting eqs. (7.18) and (7.29) into eq. (7.3):

$$w(n,y) = w_{RC}(n,y) + w_R(n,y) + w_{LC}(n,y) + w_L(n,y) \tag{7.30}$$

It should be noted that the two integrals at mid span have the property that

$$\lim_{y \to 0} (w_{RC} + w_{LC}) = -\infty .$$

This infinite downwash at the mid-span of a swept wing is a result of the kink in the vortex lines across the center line. Treatment of this problem as pertaining to the present method will be discussed in Chapter 9. The solution for the swept wing was performed by two different methods which are described in Chapters 8 and 9.

8. SWEPT WING SOLUTION WITH SERIES FOR γ DISTRIBUTION

Similar to the skewed wing, the spanwise circulation distribution is represented by a Fourier sine series. The circulation at the chordwise position $x_k = \frac{c}{2}(1 - \cos \theta_k)$ is defined as

$$\left(\frac{\gamma c}{c_R}\right)_k = \sum_{n=1}^{M-1} A_{kn} \sin n\phi_1^* \tag{8.1}$$

where $y_1 = -\frac{b}{2} \cos \phi_1^*$, and from Appendix A, for the right wing panel,

$$\phi_{1_R}^* = \cos^{-1} \left[\tfrac{1}{2} (\cos \phi_1 - 1)\right] \tag{8.2}$$

and for the left wing panel

$$\phi_{1_L}^* = \cos^{-1} \left[\tfrac{1}{2} (1 - \cos \bar{\phi}_1\right) \tag{8.3}$$

and A_{kn} are the unknown coefficients.

Defining $m_{LE} \equiv \tan \Lambda_{LE}$, $m_{TE} \equiv \tan \Lambda_{TE}$, $\Delta m \equiv m_{TE} - m_{LE} = \frac{4(\lambda-1)}{AR(\lambda+1)}$, $c_R \equiv \frac{b}{AR}$, and $\lambda \equiv \frac{c_T}{c_R}$, consider each wing panel separately. The downwash integrals for the right wing panel are given by eq. (7.18). Substitute eqs. (8.1), (8.2) and the transformed variables (see Appendix A)

$$y_1 = \frac{b}{4}(1 - \cos \phi_1) \qquad y_1 > 0 \tag{8.4}$$

$$y = \frac{b}{4}(1 - \cos \phi) \qquad y > 0 \tag{8.5}$$

$$\eta_1 = \frac{1}{2}(1 - \cos \theta_1) \tag{8.6}$$

$$\eta = \frac{1}{2}(1 - \cos \theta) \tag{8.7}$$

into eq. (7.18) and apply the midpoint trapezoidal rule to get the downwash from the right wing panel as

$$w_{RC_{i,j}} = \frac{-1}{AR(1+\lambda)N} \sum_{k=1}^{N} \sum_{n=1}^{M-1} \frac{A_{kn} \sin\left(\frac{n\pi}{2}\right) \sin \theta_k}{(1-\cos \phi_j)} K_{RC_{ijk}} \tag{8.8}$$

where $$K_{RC_{ijk}} \equiv 1 + \frac{\sqrt{\frac{1}{4}(A_1^2+1)(1-\cos \phi_j)^2 + A_1 B_1 (1-\cos \phi_j) + B_1^2}}{B_1} \tag{8.9}$$

and

$$w_{R_{i,j}} = \frac{-\pi}{2AR(1+\lambda)NM} \sum_{\ell=1}^{M} \sum_{k=1}^{N} \sum_{n=1}^{M-1} \frac{A_{kn}\, n \cdot \cos \phi^*_{\ell_R}}{(\cos \phi_\ell - \cos \phi_j)} \cdot \frac{\sin \theta_k \sin \phi_\ell}{\sin \phi^*_{\ell_R}} \cdot K_{R_{ijk\ell}} \tag{8.10}$$

with $K_{R_{ijk\ell}} \equiv 1 + \dfrac{\sqrt{\frac{1}{4}(A_1^2+1)(\cos\phi_\ell-\cos\phi_j)^2+A_1B_1(\cos\phi_\ell-\cos\phi_j)+B_1^2}}{B_1}$ (8.11)

and

$$A_1 = m_{LE} + \frac{\Delta m}{2}(1 - \cos\theta_k) \tag{8.12}$$

$$B_1 = (\cos\theta_k - \cos\theta_i)\left[\frac{2}{AR(1+\lambda)} + \frac{\Delta m}{4}(1 - \cos\phi_j)\right] \tag{8.13}$$

The downwash integrals for the left wing panel are given in eq. (7.29). Substitute eqs. (8.1), (8.3), (8.5)-(8.7), and the transformed variable (see Appendix A)

$$\bar{y}_1 = \frac{b}{4}(\cos\bar{\phi}_1 - 1) \qquad \bar{y}_1 < 0 \tag{8.14}$$

into eq. (7.29) and apply the midpoint trapezoidal rule to get the downwash from the left wing panel

$$w_{LC_{i,j}} = \frac{1}{AR(1+\lambda)N} \sum_{k=1}^{N} \sum_{n=1}^{M-1} \frac{A_{kn}\cdot\sin\left(\frac{n\pi}{2}\right)\cdot\sin\theta_k}{(1-\cos\phi_j)} \cdot K_{LC_{ijk}} \tag{8.15}$$

where $K_{LC_{ijk}} \equiv 1 + \dfrac{\sqrt{\frac{1}{4}(A_2^2+1)(1-\cos\phi_j)^2+A_2B_2(1-\cos\phi_j)+B_2^2}}{B_2}$ (8.16)

and

$$w_{L_{i,j}} = \frac{-\pi}{2AR(1+\lambda)NM} \sum_{\ell=1}^{M} \sum_{k=1}^{N} \sum_{n=1}^{M-1} \frac{A_{kn}\cdot n\cdot\cos\phi^*_{\ell_L}}{(2-\cos\phi_\ell-\cos\phi_j)} \cdot \frac{\sin\theta_k\cdot\sin\phi_\ell}{\sin\phi^*_{\ell_L}}$$

$$\cdot K_{L_{ijk\ell}} \tag{8.17}$$

where $K_{L_{ijk\ell}} \equiv 1 + \dfrac{\sqrt{\frac{1}{4}(A_2^2+1)(2-\cos\phi_\ell-\cos\phi_j)^2+A_2B_2(2-\cos\phi_\ell-\cos\phi_j)+B_2^2}}{B_2}$ (8.18)

and

$$A_2 = -\left[m_{LE} + \frac{\Delta m}{2}(1-\cos\theta_k)\right] \tag{8.19}$$

$$B_2 = \left[m_{LE} + \frac{\Delta m}{4}(2-\cos\theta_k-\cos\theta_i)\right](1-\cos\phi_j) + \frac{2}{AR(1+\lambda)}(\cos\theta_k-\cos\theta_i) \tag{8.20}$$

The control points are located at

$$\theta_i = \frac{i\pi}{N}, \quad i = 1, \ldots, N \qquad \text{(chordwise)}$$

and

$$\phi_j = \frac{j\pi}{M}, \quad j = 1, \ldots, M-1 \qquad \text{(spanwise)} \tag{8.22}$$

and the "joint" in the horseshoe vortices are located at

$$\theta_k = \frac{(2k-1)\pi}{2N}, \quad k = 1, \ldots, N \qquad \text{(chordwise)} \tag{8.23}$$

and

$$\phi_\ell = \frac{(2\ell-1)\pi}{2M}, \quad \ell = 1, \ldots, M \qquad \text{(spanwise)} \tag{8.24}$$

The downwash equation for the entire swept wing is then

$$w_{i,j} = w_{RC_{i,j}} + w_{R_{i,j}} + w_{LC_{i,j}} + w_{L_{i,j}} \tag{8.25}$$

Using the tangent flow boundary condition for thin wings given in eq. (6.22), N(M-1) values of A_{kn} are calculated by solving the matrix equation formed by applying eq. (6.22) for the chordwise and spanwise control points given by eqs. (8.21) and (8.22). It is worth noting that there is always a control point at the trailing edge which satisfies the Kutta condition. The sectional and wing aerodynamic coefficients can be calculated by using the midpoint trapezoidal rule to reduce the integrals to finite sums as shown in Chapter 9.

9. SWEPT WING SOLUTION BY DIRECT MATRIX SOLUTION FOR γ

As will be discussed in the results, the Fourier sine series for $\gamma c/c_R$ has instabilities in the solution which result from an infinite downwash at the wing centerline. To obtain a more stable solution, an alternate method is developed which solves directly for the spanwise derivative of circulation at the integration points. Thus, the unknown parameters in the matrix equation are defined as

$$A_{k\ell} \equiv \left| \frac{\partial \left(\frac{\gamma c}{c_R} \right)}{\partial \phi_\ell} \right|_{\theta_k} \tag{9.1}$$

and similar to eq. (5.16) the circulation at midspan is

$$\gamma_{k,\phi=0} = - \frac{\pi}{M} \sum_{\ell=1}^{M} A_{k,\ell} \tag{9.2}$$

The matrix equation will now contain N(M-1) equations with NM unknowns. With N(M-1) control points of eqs. (8.21) and (8.22), N more control points are needed to obtain a solution. It is known that $\frac{\partial \gamma}{\partial y_1}$ is finite at $y = 0$, thus since $y_1 = \frac{b}{4} (1 - \cos \phi_1)$

$$\left(\frac{\partial\gamma}{\partial y_1}\right)_{y=0} = \lim_{\phi_1 \to 0} \frac{\partial\gamma}{\partial\phi_1}\frac{\partial\phi_1}{\partial y_1} = \lim_{\phi_1 \to 0} \frac{\partial\gamma}{\partial\phi_1} \cdot \frac{1}{\frac{b}{4}\sin\phi_1} = \text{finite} \qquad (9.3)$$

therefore, $\left.\frac{\partial\gamma}{\partial\phi_1}\right|_{\phi_1=0} = 0$ which gives N more boundary conditions.

Define $m_{LE} \equiv \tan\Lambda_{LE}$, $m_{TE} \equiv \tan\Lambda_{TE}$, $\Delta m = m_{TE} - m_{LE} = \frac{4(\lambda-1)}{AR(\lambda+1)}$, $c_R = \frac{b}{AR}$, and $\lambda \equiv \frac{c_T}{c_R}$. Each wing panel is considered separately. The Cauchy singularity resulting from a control point being applied on the wing centerline is treated in Appendix B. The downwash integrals for the right wing panel are given in eq. (7.18). Substitute eqs. (8.5)-(8.7) and eq. (9.2) into the right wing center integral term, and replace the integral with the midpoint trapezoidal-rule sum to get

$$w_{RC_{i,j}} = \frac{\pi}{AR(1+\lambda)NM} \sum_{k=1}^{N} \sum_{\ell=1}^{M} \frac{A_{k\ell}\sin\theta_k}{(1-\cos\phi_j)} \cdot K_{RC_{ijk\ell}} \qquad (9.4)$$

$$\text{where } K_{RC_{ijk}} \equiv 1 + \frac{\sqrt{\frac{1}{4}(A_1^2+1)(1-\cos\phi_j)+A_1B_1(1-\cos\phi_j)+B_1^2}}{B_1} \qquad (9.5)$$

and A_1, B_1 are defined in eqs. (8.12) and (8.13), respectively. Substitute eqs. (8.4)-(8.7) and eq. (9.1) into the right wing panel integral term, and replace the integrals with the midpoint trapezoidal-rule sum to get

$$w_{R_{i,j}} = \frac{-\pi}{AR(1+\lambda)NM} \sum_{\ell=1}^{M} \sum_{k=1}^{N} \frac{A_{k\ell}\sin\theta_k}{\cos\phi_\ell - \cos\phi_j} \cdot K_{R_{ijk\ell}} \qquad (9.6)$$

$$\text{where } K_{R_{ijk\ell}} \equiv 1 + \frac{\sqrt{\frac{1}{4}(A_1^2+1)(\cos\phi_\ell-\cos\phi_j)^2+A_1B_1(\cos\phi_\ell-\cos\phi_j)+B_1^2}}{B_1} \tag{9.7}$$

and A_1, B_1 are defined in eqs. (8.12) and (8.13), respectively.

Considering the downwash terms of the left wing, eq. (7.29), substitute eqs. (8.5)-(8.7), and eq. (9.2) into the left wing center integral term, and replace the integral with the midpoint trapezoidal-rule sum to get

$$w_{LC_{i,j}} = \frac{-\pi}{AR(1+\lambda)NM} \sum_{k=1}^{N} \sum_{\ell=1}^{M} \frac{A_{k\ell}\cdot\sin\theta_k}{(1-\cos\phi_j)} \cdot K_{LC_{ijk}} \tag{9.8}$$

$$\text{where } K_{LC_{ijk}} \equiv 1 + \frac{\sqrt{\frac{1}{4}(A_2^2+1)(1-\cos\phi_j)^2+A_2B_2(1-\cos\phi_j)+B_2^2}}{B_2} \tag{9.9}$$

and A_2, B_2 are defined in eqs. (8.19) and (8.20), respectively. Substitute eqs. (8.5)-(8.7), eq. (8.14), and eq. (9.1) into the left wing panel integral term, and replace the integrals with the midpoint trapezoidal-rule sum to get

$$w_{L_{i,j}} = \frac{\pi}{AR(1+\lambda)NM} \sum_{\ell=1}^{M} \sum_{k=1}^{N} \frac{A_{k\ell}\cdot\sin\theta_k}{(2-\cos\phi_\ell-\cos\phi_j)} K_{L_{ijk\ell}} \tag{9.10}$$

$$\text{where } K_{L_{ijk\ell}} \equiv 1 + \frac{\sqrt{\frac{1}{4}(A_2^2+1)(2-\cos\phi_\ell-\cos\phi_j)^2+A_2B_2(2-\cos\phi_\ell-\cos\phi_j)+B_2^2}}{B_2} \tag{9.11}$$

and A_2, B_2 are defined in eqs. (8.19) and (8.20), respectively.

The control points are now located at

$$\theta_i = \frac{i\pi}{N}, \quad i = 1, \ldots, N \qquad \text{(chordwise)} \qquad (9.12)$$

and

$$\phi_j = \frac{j\pi}{M}, \quad j = 0, \ldots, M-1 \qquad \text{(spanwise)} \qquad (9.13)$$

and the "joint" in the horseshoe vortices are located at

$$\theta_k = \frac{(2k-1)\pi}{2N}, \quad k = 1, \ldots, N \qquad \text{(chordwise)} \qquad (9.14)$$

and

$$\phi_\ell = \frac{(2\ell-1)\pi}{2M}, \quad \ell = 1, \ldots, M \qquad \text{(spanwise)} \qquad (9.15)$$

The downwash equation for the entire swept wing is then

$$w_{i,j} = w_{RC_{i,j}} + w_{R_{i,j}} + w_{LC_{i,j}} + w_{L_{i,j}} \qquad (9.16)$$

Using the tangent flow boundary condition for thin wings, given in eq. (6.22), $N(M-1)$ equations are generated for control points corresponding to $i = 1, \ldots, N$ and $j = 1, \ldots, M-1$. When $j = 0$, eqs. (9.4) and (9.8) are singular. The limit of $(w_{RC_{i,j}} + w_{LC_{i,j}})$ as $\phi_j \to 0$ is approximated by, (see Appendix B)

$$(w_{RC} + w_{LC})_{i,j=0} \simeq \frac{\pi}{4NM} \sum_{\ell=1}^{M} \sum_{k=1}^{N} A_{k\ell}\, \delta_i^k \sin\theta_k \left[\frac{2(m_{LE} + \frac{\Delta m}{2}(1-\cos\theta_i))}{\cos\theta_k - \cos\theta_i} - \Delta m \right] \qquad (9.17)$$

where $$\delta_i^k = \begin{cases} +1 & \text{if } (\cos\theta_k - \cos\theta_i) > 0 \\ -1 & \text{if } (\cos\theta_k - \cos\theta_i) < 0 \end{cases} \tag{9.18}$$

This limit is actually infinite when $\Delta m \neq 0$ and $m_{LE} \neq 0$, and zero when $\Delta m = 0$ and $m_{LE} = 0$. Equation (9.17) generates N more equations if applied when $i = 1, \ldots, N$ and $j = 0$. Thus, having NM equations and NM unknowns, the $A_{k\ell}$ are calculated by solving the matrix of NM equations. It is again worth noting that there is always a control point at the trailing edge which satisfies the Kutta condition.

The sectional and wing aerodynamic characteristics may now be calculated by using the midpoint trapezoidal rule to reduce the integrals to finite sums as shown below (for swept wings)

$$\gamma_{k,j} \simeq -\frac{\pi}{M} \sum_{\ell=j+1}^{M} A_{k\ell} \tag{9.19}$$

$$(C_\ell)_j = \frac{2}{c(y)} \int_{x_{LE}}^{x_{TE}} \gamma_j(x_1)\, dx_1 \simeq \frac{\pi}{N} \sum_{k=1}^{N} \gamma_{k,j} \sin\theta_k \tag{9.20}$$

$$C_L = \frac{1}{S} \int_{-b/2}^{b/2} (C_\ell)_j\, c(y)dy \simeq \left(\frac{AR\Delta m}{8} + \frac{1}{1+\lambda}\right)\left[(C_\ell)_{j=0} + \frac{\pi^2}{NM} \sum_{k=1}^{N} \sum_{\ell=1}^{M} A_{k\ell} \sin\theta_k \cos\phi_\ell\right]$$

$$+ \frac{\Delta m AR}{16} \frac{\pi^2}{NM} \sum_{k=1}^{N} \sum_{\ell=1}^{M} A_{k\ell} \sin\theta_k \sin^2\phi_\ell \tag{9.21}$$

$$(C_m)_j = -\frac{2}{c(y)} \int_{x_{LE}}^{x_{TE}} \gamma_j(x_1) x_1 dx_1 \simeq -\frac{\pi}{2N} \sum_{k=1}^{N} \gamma_{k,j} (1-\cos\theta_k) \sin\theta_k \tag{9.22}$$

$$C_M = \frac{1}{Sc} \int_{-b/2}^{b/2} (C_m)_j \, c^2(y)dy \simeq \left[\frac{\Delta m AR}{8} + \frac{1}{(1+\lambda)}\right]\left[(C_m)_{j=0}\right.$$

$$\left. - \frac{\pi^2}{2NM} \sum_{k=1}^{N} \sum_{\ell=1}^{M} A_{k\ell} (1-\cos\theta_k) \sin\theta_k \cos\phi_\ell\right]$$

$$- \frac{\Delta m AR}{32} \frac{\pi^2}{NM} \sum_{k=1}^{N} \sum_{\ell=1}^{M} A_{k\ell}(1-\cos\theta_k) \sin\theta_k \sin^2\phi_\ell$$

(9.23)

10. RESULTS AND DISCUSSION

10.1 Prandtl's Lifting Line Equation

Figure 4 illustrates the convergence of this method compared with the Multhopp series (Fourier sine series) method of reference 7 and the conventional VLM (ref. 3) for C_{L_α} of a rectangular planforms with an aspect ratio of 2π. Prandtl's lifting line theory requires trailing vortices and spanwise control points, but no chordwise control points are needed because the theory assumes the downwash is constant in the chordwise direction. Therefore, the control points are placed on the "bound" vortex for both methods. In this way, the accuracy of the spanwise vortex arrangement can be observed without the influence of the location of chordwise control points. Figure 4 shows that the present method converges very quickly and approaches the correct limit as does the Multhopp series method. Figure 4 shows that the conventional VLM converges slowly and C_{L_α} does not appear to approach the correct limit when the curve is extrapolated to an infinite number of trailing vortices, $M \to \infty$ $(1/M \to 0)$.

Figure 5 shows the distribution of circulation over the span for a variation of the number of trailing vortices. The circulation distribution remains virtually unchanged as the number of vortices increases from M = 2 to M = 10.

10.2 Skewed Wing

Table I gives a comparison of the results of the present method with the conventional VLM, (ref. 3), for two skewed wings with $\Lambda_{LE} = 30°$, $\lambda = 1.0$ and AR = 1.0 and 1.5. The vortex lattice method is applied for 4 chordwise and 12 spanwise integration points. The results for the VLM are linearly interpolated to correspond with the present method results. This table shows that the spanwise variation of the sectional life coefficient compares reasonably well with the VLM. The spanwise lift distribution is illustrated in Figure 6 for AR = 1.5. The distribution is non-symmetrical which is characteristic of skewed wings.

The lift-curve slope is slightly lower than the VLM although the two are in good agreement. The moment coefficient and aerodynamic center location compares reasonably well with the VLM for the AR = 1.5 wing, but the comparison is poor for the AR = 1.0 wing.

10.3 Swept Wing

The downwash equation for the swept wing yields an infinitely large downwash at any spanwise location where a discontinuity, or kink, exists in the spanwise (bound) vortex lines (ref. 11). For the linear taper swept wing, a kink exists at the centerline ($y = 0$) resulting in an infinitely large dowewash at $y = 0$, which is unrealistic. This infinite downwash at the centerline causes computational problems with the direct-

matrix method because control points are located at y = 0. As discussed in ref. 11, the mathematical model of eq. (9.1) is not accurate at the midspan of the swept wing. One way to resolve this problem too is to round the leading and trailing edges near the midspan point. However, the infinite downwash does not appear directly with the Fourier sine series method since no control points lie on the wing centerline. On the other hand, it does cause serious instabilities in the solution as the number of spanwise control points increase because control points are approaching y = 0. The rectangular wing presents no problems for the method with respect to the infinite downwash at y = 0 since no kinks exist in the spanwise vortex-lines and hence no infinite downwash.

Table 2(a) and Figure 7 give a comparison of the results of the Fourier sine-series method to those of the direct-matrix method for a 45° swept wing of AR = 2.0 and λ = 1.0. Figure 7 shows an increasing oscillation of the sectional lift coefficient in the spanwise direction for the Fourier sine-series method. This oscillation is attributed to the control points near the centerline of the wing being affected by the infinitely large downwash at the centerline, thus introducing a numerical instability into the solution. It is significant to note that the direct-matrix method yields a very reasonable spanwise variation of sectional lift coefficient. Table 2(a) shows that the lift curve slope for the sine-series method and the direct-matrix method compare very closely, but both values are slightly lower than the lift curve slope calculated by the VLM (ref. 3).

Table 2(b) gives a comparison between the lift curve slopes for the direct-matrix method and the VLM for a 45° swept wing with taper ratios of 0.0 and 0.5 and aspect ratios of 2.0, 4.5, and 7.0. The present method

gives very unsatisfactory results for C_{L_α} for swept wings with taper. The error in C_{L_α} increases as the taper ratio decreased from 1 to 0. The error is attributed to the infinite downwash at midspan, and a satisfactory solution would require rounding the leading and trailing edges near midspan as done in reference 11.

10.4 Rectangular Wing

The terms in the downwash equation which causes the infinite downwash at y = 0 for the swept wing vanish in the case of constant taper and zero sweep. This result is expected since the rectangular wing has no kinks in the vortex lines. Table 3 presents the results for a rectangular wing, AR = 2. Table 3(a) gives a comparison of the results of the Fourier sine-series method to those of the direct-matrix method for the variation in the spanwise sectional lift coefficient. The two methods are in very close agreement. This adds basis to the hypothesis that the spanwise oscillation of the swept wing sectional lift coefficient using the Fourier sine-series method is attributed to the infinite downwash at y = 0, which causes numerical instability in the solution. Table 3(b) shows that the direct-matrix method yields a variation of sectional lift coefficient very close to that of reference 7. Some difference in the two methods may be as a result of the quadratic interpolation method used to obtain the comparable sectional lift coefficients. Table 3 also shows that the direct matrix method gives the same overall aerodynamic coefficients as those in reference 7. The results for the overall aerodynamic coefficients for the Fourier sine-series method do not compare as well as the direct matrix method. The major difference between the present methods and the method of ref. 7 is that the present methods

apply the semi-circle distribution of control points and integration points over the two half spans and the method of ref. 7 applies the semi-circle distribution over the whole span.

10.5 Compressibility Effects

All of the results given in this report are for incompressible flow. Subsonic compressibility effects may be included very simply by applying the Prandtl-Glauret rule (ref. 3).

10.6 Computational Requirements

The examples computed herein were all performed on an IBM 370/165 computer. Typical cases for the lifting surface theory required about 20 seconds of CPU time.

11. CONCLUSIONS

The following conclusions are drawn from the present investigation:

1. The new lifting-surface method developed herein was found to compare well with other lifting-surface theories, but with much smaller computational times.
2. This new method is more accurate and converges faster than conventional vortex lattice methods.
3. For skewed and rectangular wings, the results using the Fourier-sine series for the spanwise variation of circulation are essentially the same as those using the direct matrix solution.
4. For swept wings, considerable differences were found in the results using the Fourier-sine series as compared to the direct matrix solution. The Fourier-sine series method was found to give an oscillatory solution

for the circulation, and the amplitude increased as more terms were included in the series. The direct matrix solution was found to give more satisfactory results.

5. The basic equation used in lifting surface theories gives an infinite downwash at the midspan of swept wings. This singularity in the equation is caused by the "kink" at midspan in the spanwise vortices, and the effects of it can be minimized by positioning control points away from the midspan position. Another alternative is to round the leading and trailing edges near midspan, thereby eliminating the kinks in the spanwise vortices.

APPENDIX A

Transformations for Swept Wings

The present method uses the "semi-circle" coordinate system for the spanwise and chordwise direction. The "semi-circle" method is applied separately to the right and left wing panels for the swept wing because of a kink at the midspan, (see figure A-1). The transformation from (η,y) to (θ,ϕ) is made by introducing the transformations:

Chordwise Direction

$$\eta = \frac{1}{2}(1 - \cos\theta) \quad \text{control point} \tag{A-1}$$

$$\eta_1 = \frac{1}{2}(1 - \cos\theta_1) \quad \text{vortex point} \tag{A-2}$$

where

$\theta = 0$ at $\eta = 0$ (leading edge)

$\theta = \pi$ at $\eta = 1$ (trailing edge)

Spanwise Direction

Right-Wing Panel: $y = \frac{b}{4}(1 - \cos\phi)$ control point (A-3)

$$y_1 = \frac{b}{4}(1 - \cos\phi_1) \quad \text{vortex point} \tag{A-4}$$

where

$\phi = 0$ at $y = 0$

$\phi = \pi$ at $y = \frac{b}{2}$

Left-Wing Panel: $\bar{y}_1 = \frac{b}{4}(\cos \bar{\phi}_1 - 1)$ vortex point (A-5)

where

$$\bar{\phi}_1 = 0 \quad \text{at} \quad \bar{y}_1 = 0$$

$$\bar{\phi}_1 = \pi \quad \text{at} \quad \bar{y}_1 = -\frac{b}{2}$$

The control points are only applied to the right wing panel because of symmetry, thus, eq. (A-3) applies for the left wing panel integration also.

For the case where circulation is represented by a Fourier sine series, it is necessary to transform the half-span "semi-circle" coordinate system into a full span "semi-circle" coordinate system. This is accomplished by defining for the right wing panel

$$\phi^*_{1_R} = \cos^{-1} [\tfrac{1}{2}(\cos \phi_1 - 1)] \tag{A-6}$$

where

$$\phi^*_{1_R} = \frac{\pi}{2} \quad \text{at} \quad \phi_1 = 0, \; y = 0$$

$$\phi^*_{1_R} = \pi \quad \text{at} \quad \phi_1 = \pi, \; y = +\frac{b}{2}$$

and for the left wing panel

$$\phi^*_{1_L} = \cos^{-1} [\tfrac{1}{2}(1 - \cos \bar{\phi}_1)] \tag{A-7}$$

where

$$\phi^*_{1_L} = \frac{\pi}{2} \quad \text{at} \quad \bar{\phi}_1 = 0, \; y = 0$$

$$\phi^*_{1_L} = 0 \quad \text{at} \quad \bar{\phi}_1 = \pi, \; y = -\frac{b}{2}$$

APPENDIX B

Singularities at Midspan of Swept Wings

Singularities occur in eqs. (6.21) and (6.33) when $y \to y_1$, $y \to \bar{y}_1$, and $y \to 0$. These Cauchy singularities are treated using Lan's approach (ref. 4). The downwash equation for the right wing panel in integral form is

$$w_R = -\frac{c_R}{2\pi} \int_0^{\pi} \int_0^{\pi} \left[\frac{\partial\left(\frac{\gamma c}{c_R}\right)}{\partial \phi_1}\right]_{\theta_1} \frac{\sin \theta_1 \cdot \bar{K}_R}{(\cos \phi_1 - \cos \phi)} \, d\theta_1 \, d\phi_1 \tag{B-1}$$

where $$\bar{K}_R \equiv 1 + \frac{\sqrt{\frac{1}{4}(\bar{A}_1^2+1)(\cos \phi_1 - \cos \phi)^2 + \bar{A}_1 \bar{B}_1 (\cos \phi_1 - \cos \phi) + \bar{B}_1^2}}{\bar{B}_1} \tag{B-2}$$

and

$$\bar{A}_1 = m_{LE} + \frac{\Delta m}{2}(1 - \cos \theta_1) \tag{B-3}$$

$$\bar{B}_1 = (\cos \theta_1 - \cos \theta)\left[\frac{2}{AR(1+\lambda)} + \frac{\Delta m}{4}(1 - \cos \phi)\right] \tag{B-4}$$

Integrating (B-1) in the spanwise direction

$$\int_0^{\pi} \left[\frac{\partial\left(\frac{\gamma c}{c_R}\right)}{\partial \phi_1}\right] \frac{\bar{K}_R(\phi, \phi_1) \, d\phi_1}{(\cos \phi_1 - \cos \phi)} = \int_0^{\pi} \frac{\left[\frac{\partial\left(\frac{\gamma c}{c_R}\right)}{\partial \phi_1}\right] \cdot \bar{K}_R(\phi, \phi_1) - \left[\frac{\partial\left(\frac{\gamma c}{c_R}\right)}{\partial \phi}\right] \cdot (2)}{\cos \phi_1 - \cos \phi} d\phi_1$$

$$\simeq \frac{\pi}{M} \sum_{\ell=1}^{M} \frac{\left[\frac{\partial\left(\frac{\gamma c}{c_R}\right)}{\partial \phi_\ell}\right] \cdot \bar{K}_{R_{ijk\ell}}}{\cos \phi_\ell - \cos \phi_j} + \begin{cases} 2\pi M \left[\frac{\partial\left(\frac{\gamma c}{c_R}\right)}{\partial \phi}\right]_k & , j = 0 \\ 0 & , j \neq 0 \\ 0 & , j = M \end{cases} \tag{B-5}$$

where

$$\phi_\ell = \frac{(2\ell-1)\pi}{2M}, \qquad \ell = 1, \ldots, M \qquad \text{(spanwise)} \qquad \text{(B-6)}$$

and

$$\phi_j = \frac{j\pi}{M}, \qquad j = 0,1, \ldots, M-1 \qquad \text{(spanwise)} \qquad \text{(B-7)}$$

It is known that $\frac{\partial \gamma}{\partial y_1}$ is finite at $y = 0$, thus since $y_1 = \frac{b}{4}(1-\cos \phi_1)$,

$$\left(\frac{\partial \gamma}{\partial y_1}\right)_{y=0} = \lim_{\phi_1 \to 0} \frac{\partial \gamma}{\partial \phi_1} \frac{\partial \phi}{\partial y_1} = \lim_{\phi_1 \to 0} \frac{\partial \gamma}{\partial \phi_1} \frac{4}{b \sin \phi_1} = \text{finite}$$

therefore

$$\left.\frac{\partial \gamma}{\partial \phi_1}\right|_{\phi_1=0} = 0 \qquad \text{(B-8)}$$

This shows the extreme right side term of eq. (B-5) to be zero when $j = 0$, thus eq. (B-5) becomes

$$\int_0^\pi \left[\frac{\partial\left(\frac{\gamma c}{c_R}\right)}{\partial \phi}\right] \frac{K_R(\phi,\phi_1)\,d\phi_1}{(\cos \phi_1 - \cos \phi)} = \frac{\pi}{M} \sum_{\ell=1}^{M} \frac{\left[\frac{\partial\left(\frac{\gamma c}{c_R}\right)}{\partial \phi_\ell}\right] K_{R_{ijk\ell}}}{\cos \phi_\ell - \cos \phi_j} \qquad \text{(B-9)}$$

where

$$K_{R_{ijk\ell}} \equiv 1 + \frac{\sqrt{\frac{1}{4}(A_1^2+1)(\cos \phi_\ell - \cos \phi_j)^2 + A_1 B_1 (\cos \phi_\ell - \cos \phi_j) + B_1^2}}{B_1} \qquad \text{(B-10)}$$

Therefore, replacing eq. (B-1) by the midpoint trapezoidal-rule sum to get the downwash from the right wing panel

$$w_{R_{i,j}} = \frac{-\pi}{AR(1+\lambda)NM} \sum_{\ell=1}^{M} \sum_{k=1}^{N} \frac{A_{k\ell} \cdot \sin \theta_k}{\cos \phi_\ell - \cos \phi_j} \cdot \overline{K}_{R_{ijk\ell}} \tag{B-11}$$

where

$$A_{k_\ell} \equiv \left[\frac{\partial \left(\frac{\gamma c}{c_R} \right)}{\partial \phi_\ell} \right]_{\theta_k} \tag{B-12}$$

The significant result is that eq. (B-11) applies for control points $j = 0, \ldots, M - 1$, giving NM equations with NM unknowns.

It can be shown similarly by using Lan's method for treating Cauchy singularities that the downwash from the left wing panel is

$$w_{L_{i,j}} = \frac{\pi}{AR(1+\lambda)NM} \sum_{\ell=1}^{M} \sum_{k=1}^{N} \frac{A_{k\ell} \sin \theta_k}{(2 - \cos \phi_\ell - \cos \phi_j)} \cdot K_{L_{ijk\ell}} \tag{B-13}$$

$$\text{where } K_{L_{ijk\ell}} \equiv 1 + \frac{\sqrt{\frac{1}{4}(A_2^2+1)(2-\cos \phi_\ell - \cos \phi_j)^2 + A_2 B_2 (2 - \cos \phi_\ell - \cos \phi_j) + B_2^2}}{B_2} \tag{B-14}$$

and the integration points and control points are given in eqs. (B-6) and (B-7) respectively.

The center integral terms of eqs. (6.21) and (6.33) have a singularity as $y \to 0$. Add the center integral terms to get

$$w_{LC} + w_{RC} = \frac{c_R}{4\pi} \int_0^1 \frac{\gamma(\eta_1, 0)}{y} \left[\frac{\sqrt{Y_0'}}{B'} - \frac{\sqrt{Y_0}}{B} \right] d\eta_1 \tag{B-15}$$

The limit of this equation as $y \to 0$ is

$$\lim_{y \to 0} (w_{LC}+w_{RC}) = \frac{1}{4\pi} \int_0^1 \gamma(\eta_1,0) \left[2\Delta m \frac{|\eta-\eta_1|}{(\eta-\eta_1)} - 2(m_{LE}+\Delta m\eta) \frac{|\eta\ \eta_1|}{(\eta-\eta_1)^2} \right] d\eta_1 \quad \text{(B-16)}$$

where $\eta = \frac{1}{2}(1-\cos\theta)$, $d\eta_1 = \frac{1}{2} \sin\theta_1\, d\theta_1$.

Consider the integral

$$\int_0^1 \frac{|\eta-\eta_1|}{(\eta-\eta_1)^2}\, d\eta_1 = \int_0^\pi \frac{|\cos\theta_1-\cos\theta|}{(\cos\theta_1-\cos\theta)^2} \sin\theta_1\, d\theta_1$$

$$= \lim_{\varepsilon \to 0} \left[\int_0^{\theta-\varepsilon} \frac{\sin\theta_1}{\cos\theta_1-\cos\theta}\, d\theta_1 - \int_{\theta+\varepsilon}^{\pi} \frac{\sin\theta_1\, d\theta_1}{\cos\theta_1-\cos\theta} \right]$$

$$= \lim_{\varepsilon \to 0} \left\{ \frac{1}{\sin\theta} \left[\log \sin\left(\theta - \tfrac{1}{2}\varepsilon\right) - \log \sin \tfrac{1}{2}\varepsilon \right] \right.$$

$$\left. - \frac{1}{\sin\theta} \left[\log \sin \tfrac{1}{2}\varepsilon - \log \sin\left(\theta + \tfrac{1}{2}\varepsilon\right) \right] \right\}$$

$$= -\infty \quad \text{(B-17)}$$

Thus, the downwash at the center $y = 0$ is infinite for a swept or tapered wing. Note, however, that when $m_{LE} = 0$ and $\Delta m = 0$, i.e., a rectangular wing, the limit of eq. (B-16) is zero.

For computational purposes, eq. (B-16) is replaced by the midpoint trapezoidal rule sum to get

$$(w_{RC}+w_{LC})_{j=0} \simeq \frac{\pi}{4NM} \sum_{\ell=1}^{M} \sum_{k=1}^{N} A_{k\ell}\, \delta_i^k \sin\theta_k \left[\frac{2(m_{LE}+\frac{\Delta m}{2}(1-\cos\theta_i))}{\cos\theta_k-\cos\theta_i} - \Delta m \right]$$

where

$$\delta_i^k = \begin{cases} +1 & \text{if } (\cos\theta_k - \cos\theta_i) > 0 \qquad \text{(B-18)} \\ -1 & \text{if } (\cos\theta_k - \cos\theta_i) < 0 \qquad \text{(B-19)} \end{cases}$$

12. REFERENCES

1. Griffith, S. L., "An Experimental Investigation of Favorable Interference Effects from a Wing and Proprotor," M.S. Thesis, N. C. State University, Raleigh, N. C. (April, 1976).
2. Griffith, S. L., DeJarnette, F. R. and Murray, J. J., "An Experimental Investigation of Favorable Interference Effects from a Wing and Proprotor," (Proceedings of AIAA 3rd Atmospheric Flight Mechanics Conference, Arlington, Texas, June 7-9, 1976), pp. 92-100.
3. Margason, R. J. and Lamar, J. E., "Vortex-Lattice Fortran Program for Estimating Subsonic Aerodynamic Characteristics of Complex Planforms," NASA TN D-6142 (1971).
4. Lan, C. E., "A Quasi-Vortex Lattice Method in Thin Wing Theory," J. Aircraft, Vol. 11, No. 9, pp. 518-527 (1974).
5. Thwaites, B. (editor), Incompressible Aerodynamics (Oxford at the Clarendon Press, England, 1960).
6. Hough, G. R., "Remarks on Vortex-Lattice Methods," J. Aircraft, Vol. 10, No. 5, pp. 314-317 (1973).
7. DeJarnette, F. R., "Arrangement of Vortex Lattices on Subsonic Wings," NASA SP-405, pp. 301-324, (1976).
8. DeJarnette, F. R., "Lifting Surface Theory for Rectangular Wings," NASA CP-2001, Vol. 4, pp. 1301-1310 (1976).
9. Keuthe, A. M. and Chow, C., Foundations of Aerodynamics (John Wiley and Sons, New York, 1976), 3rd ed., Chapter 5.
10. Ashley, H. and Landahl, M. T., Aerodynamics of Wings and Bodies (Addison-Wesley Publishing Co., New York, 1965), Chapter 7.
11. Garner, H. C., Hewitt, B. L. and Labrujere, T. E., "Comparison of Three Methods for the Evaluation of Subsonic Lifting Surface Theory," Reports and Memoranda 3597, Aeronautical Research Council, London, England (1968).

TABLE 1. Results for Skewed Planforms
$\Lambda_{LE}=30°$, $\lambda=1.0$, AR=1.5 and 1.0

Values of C_ℓ/C_L

AR=1.5

2y/b	Present N=4, M=12	VLM (ref. 3) N=6, M=40
0.9659	0.3517	0.4032
0.8660	0.6742	0.6908
0.7071	0.9416	0.9423
0.5000	1.1339	1.1258
0.2588	1.2408	1.2276
0	1.2620	1.2464
-0.2588	1.2032	1.2003
-0.5000	1.0718	1.0608
-0.7071	0.8748	0.8719
-0.8660	0.6209	0.6331
-0.9659	0.3230	0.3682

AR=1.0

2y/b	Present N=4, M=12	VLM (ref. 3) N=6, M=40
0.9659	0.3390	0.3884
0.8660	0.6528	0.6683
0.7071	0.9184	0.9185
0.5000	1.1172	1.1085
0.2588	1.2363	1.2227
0	1.2698	1.2544
-0.2588	1.2186	1.2042
-0.5000	1.0880	1.0778
-0.7071	0.8869	0.8850
-0.8660	0.6274	0.6406
-0.9659	0.3252	0.3715

Overall Values

	Present	VLM
C_{L_α}	1.9629	2.0057
$-C_{M_\alpha}$	0.4120	0.4417
Xac/c	0.2048	0.2202

	Present	VLM
C_{L_α}	1.4399	1.4736
$-C_{M_\alpha}$	0.2581	0.1546
Xac/c	0.1793	0.1049

TABLE 2. Results for 45° Swept Wing
AR=2.0, λ=1.0

(a)

Values of C_ℓ/C_L

N=4, M=12

2y/b	Sine Series Method	Non-Series Method
0.0170	1.1515	1.1550
0.0670	1.1595	1.1623
0.1464	1.1699	1.1719
0.2500	1.1794	1.1775
0.3706	1.1547	1.1660
0.5000	1.1557	1.1250
0.6294	0.9611	1.0430
0.7500	1.0740	0.9130
0.8536	0.4839	0.7349
0.9330	0.7937	0.5152
0.9830	0.0749	0.2655

Overall Values of C_{L_α}

	Sine Series Method	Direct Matrix Method	VLM (ref. 3)
C_{L_α}	2.2544	2.2586	2.265

(b)

Swept, Tapered Wing
Λ_{LE}=45°

N=4 M=12		C_{L_α}	
AR	λ	Direct Matrix Method	VLM (ref. 3)
2.0	0.5	2.6463	2.4408
4.5	0.5	3.6774	3.3690
7.0	0.5	4.0393	3.7013
2.0	0.0	9.3418	2.3606
4.5	0.0	11.7134	3.4779

TABLE 3. Results for Rectangular Wing

AR=2.0

Values of C_ℓ/C_L

a) Comparison of Fourier Sine-Series Method to Direct Matrix Method

N=4, M=8

2y/b	Sine Series Method	Direct Matrix Method
0.0381	1.2535	1.2539
0.1464	1.2424	1.2437
0.3087	1.2000	1.2023
0.5000	1.1028	1.1059
0.6913	0.9324	0.9358
0.8536	0.6820	0.6850
0.9619	0.3618	0.3636

b) Comparison of Direct Matrix Method to Method of Reference 7

N=4, M=8

2y/b	Direct Matrix Method (Interpolated)	Method of ref. 7
0	1.2543	1.2543
0.1951	1.2301	1.2335
0.3827	1.1640	1.1706
0.5556	1.0576	1.0651
0.7071	0.9126	0.9171
0.8315	0.7237	0.7290
0.9239	0.4997	0.5084
0.9808	0.2575	0.2618

Overall Values

	Sine Series Method	Direct-Matrix Method	Method of ref. 7
C_{L_α}	2.4733	2.4732	2.4732
$-C_{M_\alpha}$	0.5143	0.5187	0.5187
x_{ac}/C	0.2079	0.2097	0.2097

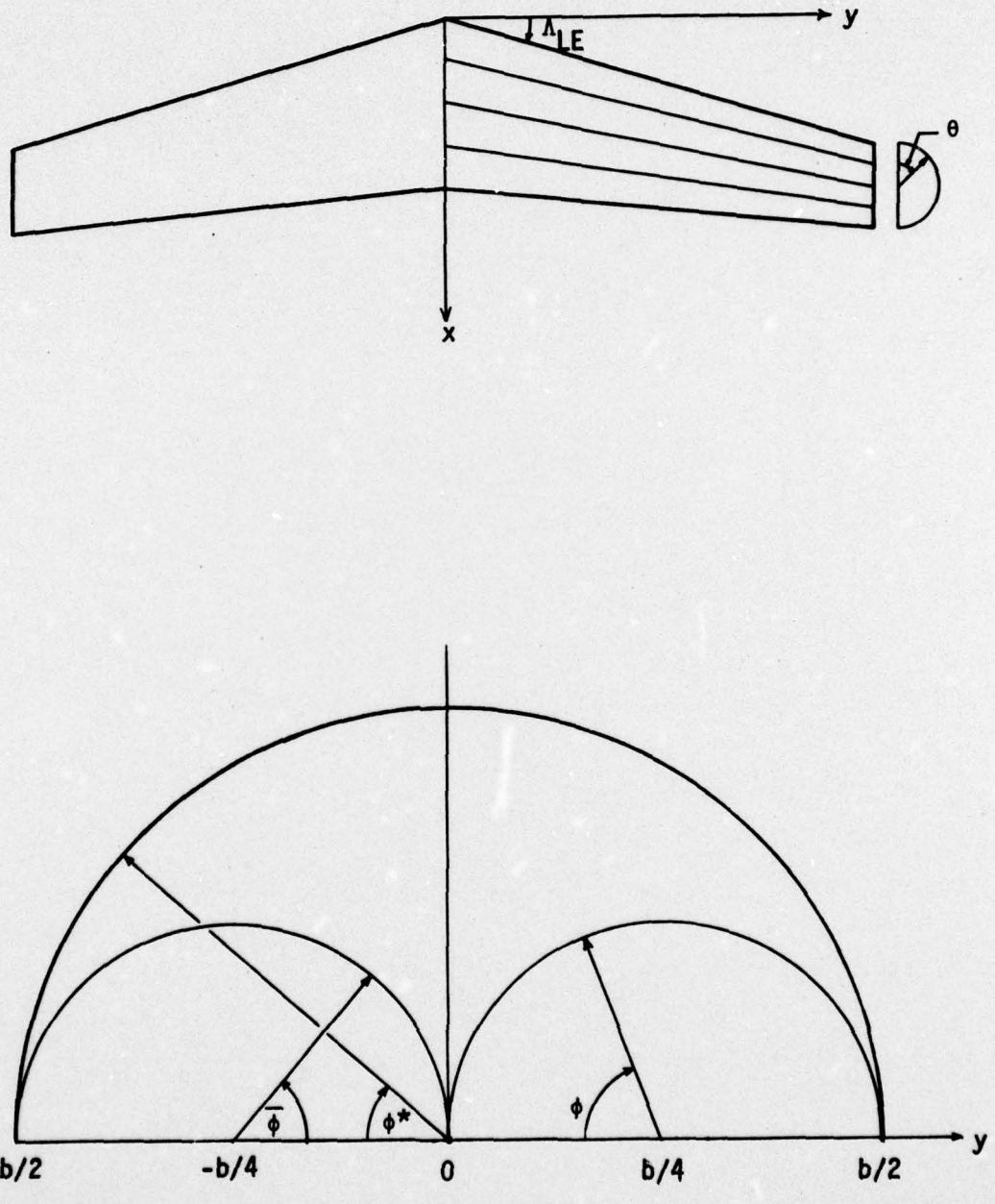

FIGURE A-1. Chordwise and Spanwise "Semi-Circle" Transformations.

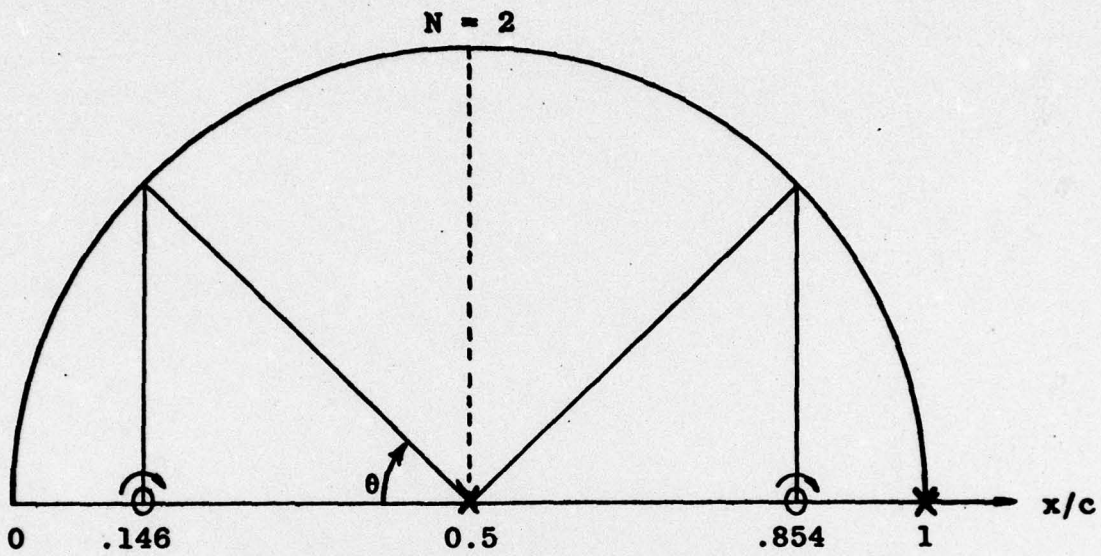

$$x/c = (1 - \cos\theta)/2$$

O Vortex Position: $\theta_k = \frac{(2k - 1)\pi}{2N}$ $(k = 1, \ldots, N)$

X | Control Points : $\theta_i = \frac{i\pi}{N}$ $(i = 1, \ldots, N)$

Figure 1. Lan's vortex arrangement for airfoils.

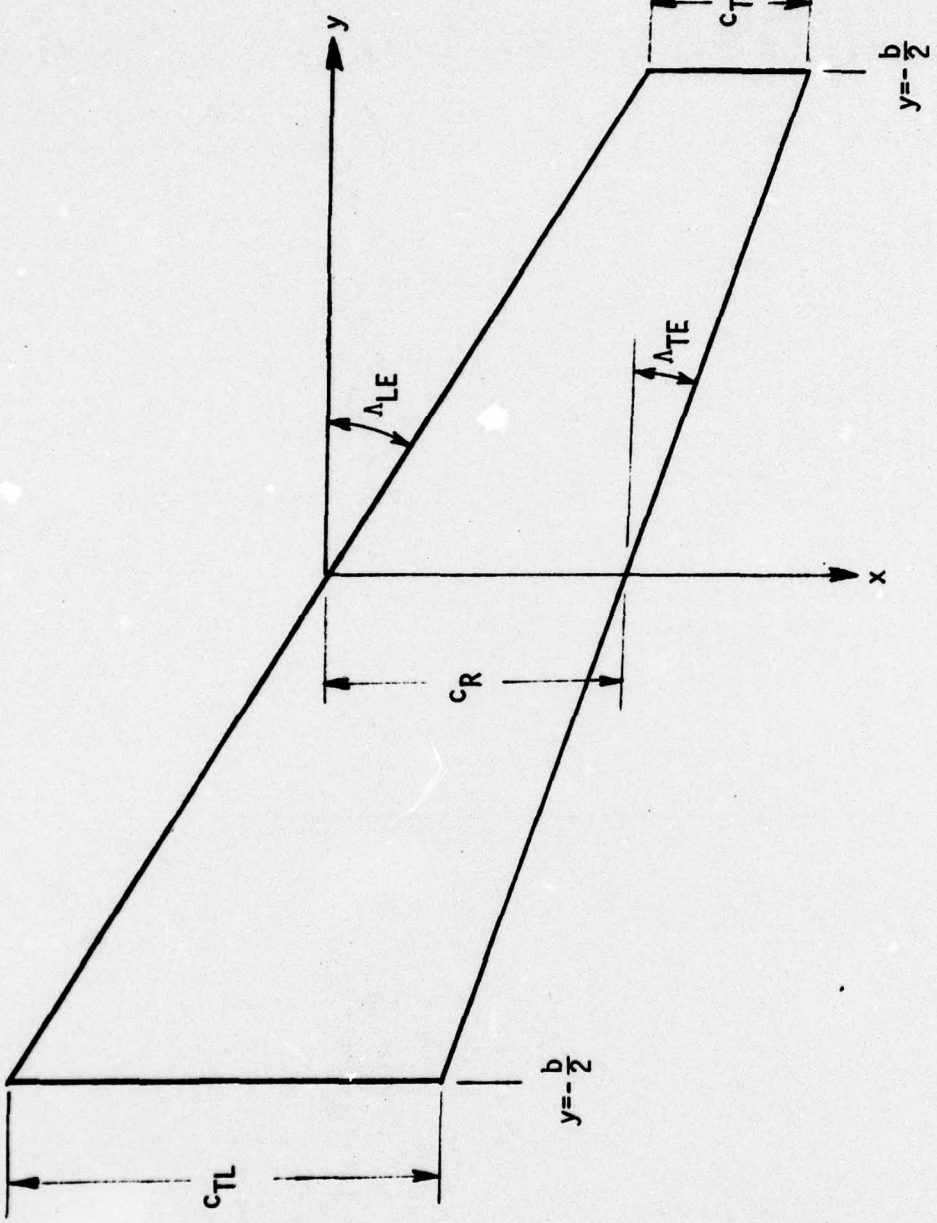

FIGURE 2. Geometry and Coordinate System for Skewed Wing

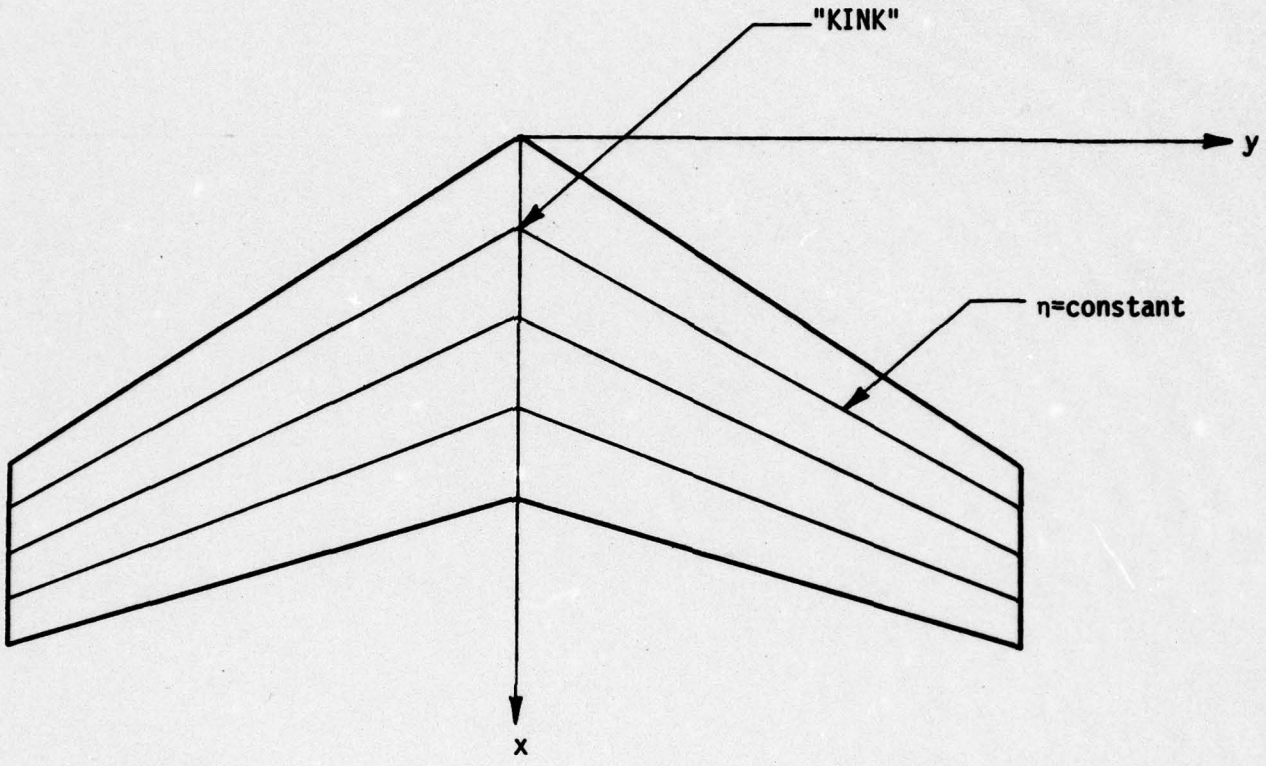

FIGURE 3. Spanwise Vortex Line Geometry of Swept Wing

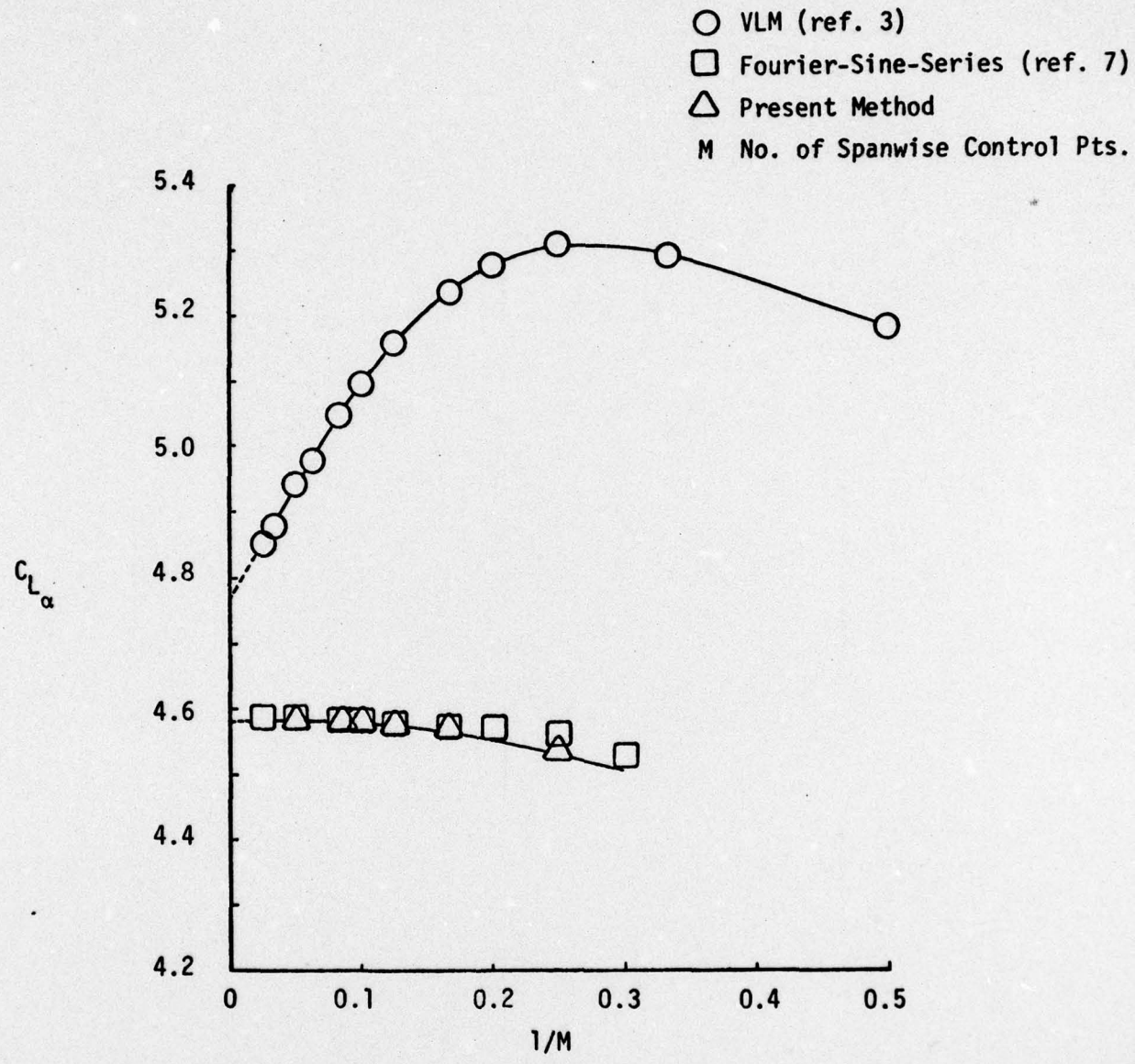

FIGURE 4. Convergence of C_{L_α} Predicted by Three Methods of Solving Prandtl's Lifting-Line Equation, Rectangular Wing, AR=2π.

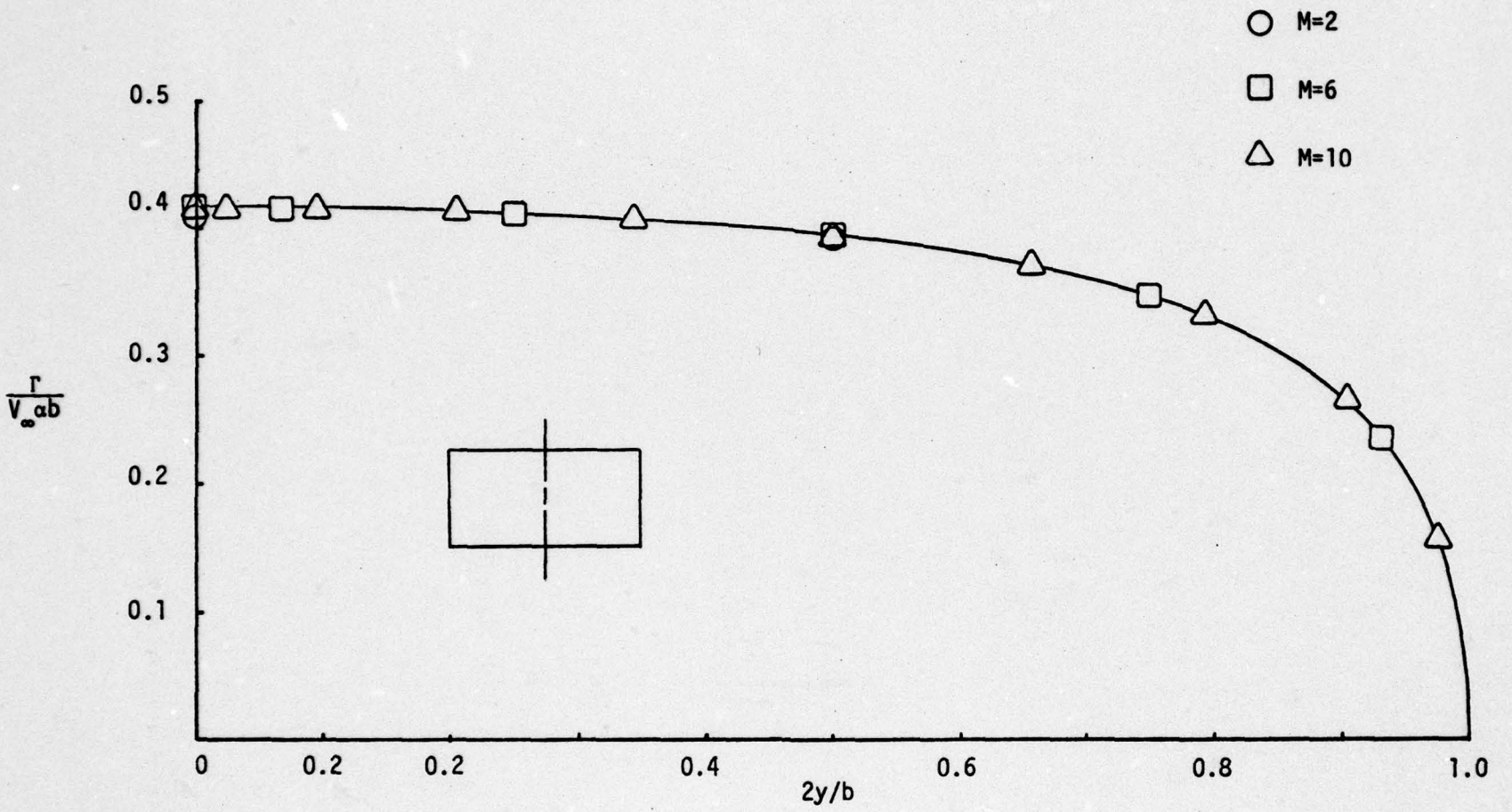

FIGURE 5. Effect of Number of Spanwise Control Points on Circulation of Rectangular Wing, AR=2π, . From Prandtl's Lifting-Line Equation.

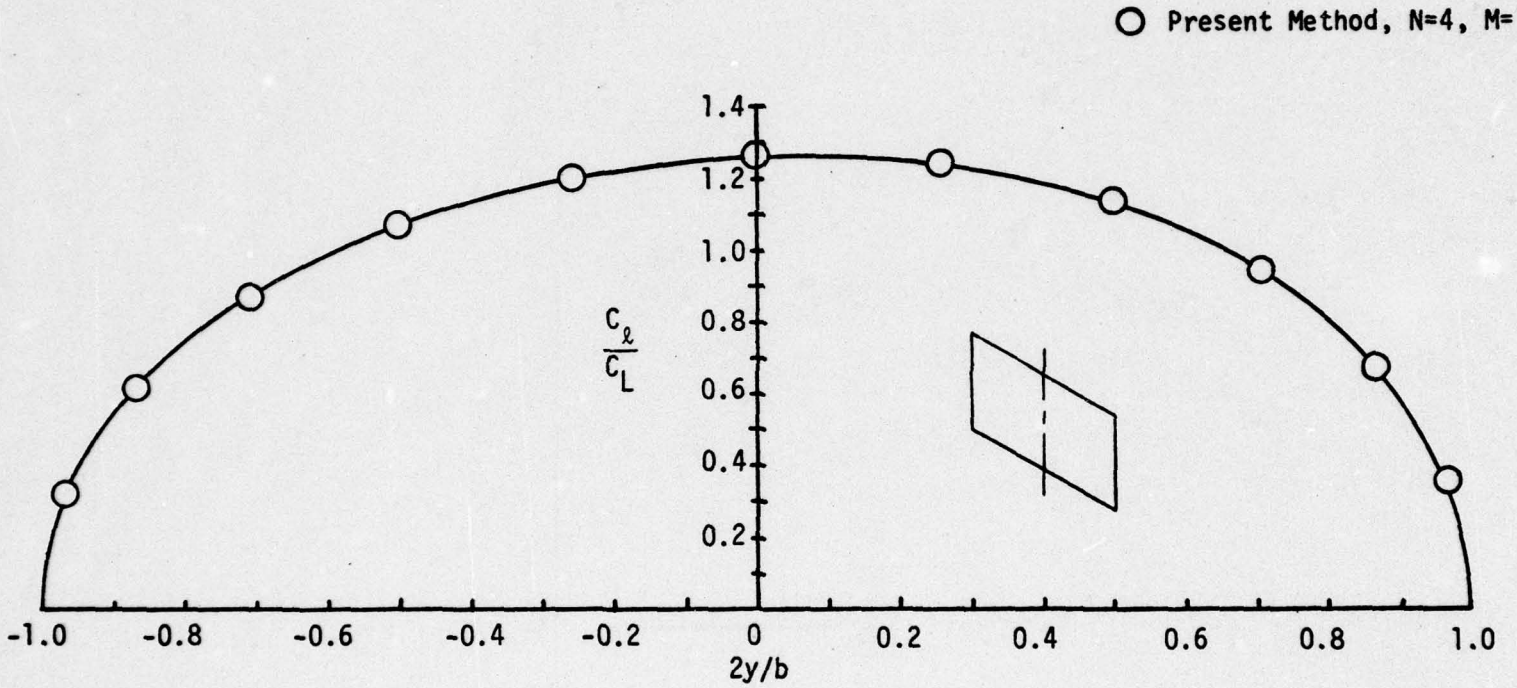

FIGURE 6. Lift Distribution for Skewed Wing, Λ_{LE}=30°, AR=1.5, λ=1.

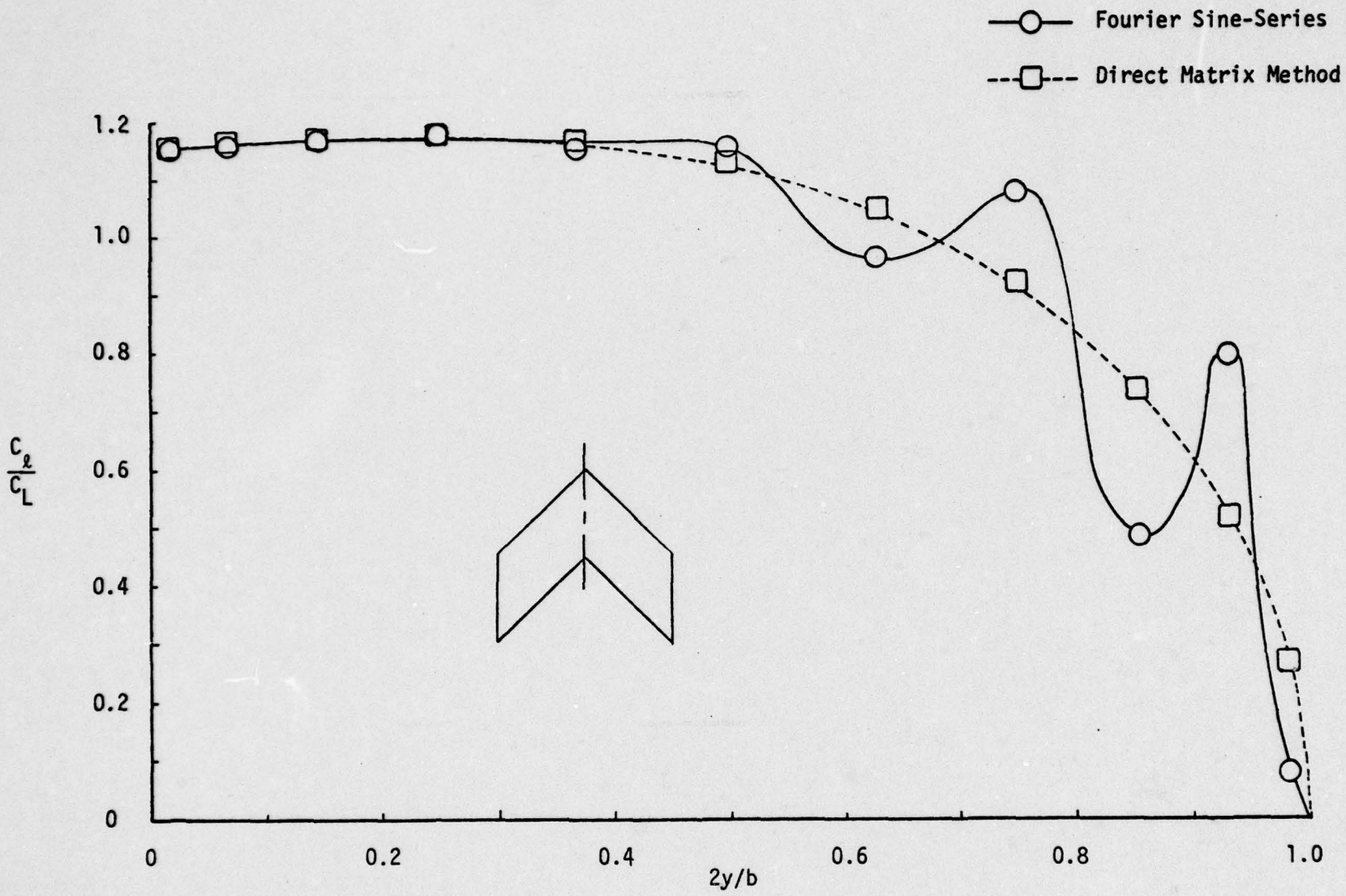

FIGURE 7. Lift Distribution on 45° Swept Wing, AR=2, λ=1.